

Rob Pywell

RAYTRACE

S. Kowalski and H.A. Enge

Laboratory for Nuclear Science
and
Department of Physics
Massachusetts Institute of Technology
Cambridge, Massachusetts 02139 U.S.A.

May 16, 1986

TABLE OF CONTENTS

Abstract

I. Introduction

II. General Ion Optics

III. Ray Tracing

IV. General Routines

- A. MAIN
- B. RAYS
- C. OPTIC
- D. PRNT
- E. MATRIX
- F. MTRX1
- G. DERIV
- H. FNMIRK
- I. PLTOUT

V. Element Routines

- A. DIPOLE Magnetic Dipole
 - 1. MTYP = 1 Homogenous-Field Dipole: General Description
 - 2. MTYP = 2 Homogenous-Field Dipole
 - 3. MTYP = 3 Dipole with Field Gradient
 - 4. MTYP = 4 Dipole with Field Gradient
 - 5. MTYP = 5 Circular-Pole Dipole
 - 6. MTYP = 6 Pretzel Magnet
- B. EDIPL Electrostatic Cylinder Deflector
- C. POLES Multipole (Quadrupole, etc.)
- D. MULT Multipole Corrector
- E. SOLND Solenoid
- F. VELs Velocity Selector
- G. LENS Transformation Matrix
- H. SHRT Shift-Rotate
- I. DRIFT Field-Free Drift
- J. COLL Collimator

References

Appendix 1. Input Parameter Description

Appendix 2. Samples of Input Data Files

I. Introduction

A very general ion-optical computer code called RAYTRACE has been developed at MIT during the last twenty years. Originally it was limited to a treatment of optics of uniform-field dipole magnets. It has since been expanded and modified many times. It now includes routines for non-uniform magnets of various kinds, solenoids, Wien filters ($E \times B$), electrostatic deflectors, and multipoles up to dodecapole. A routine for an accelerator section is not supported at present.

The ion-optical code TRANSPORT¹ is widely used for designing beam transport systems. This program calculates first and second order transfer coefficients (matrix elements) for the beam parameters position and slope. It is a fast program with fitting routines that adjust variable field strengths, drifts, angles, curvatures, etc., to produce specified focusing effects. RAYTRACE does not replace or compete with TRANSPORT. Indeed, users of RAYTRACE practically always start with TRANSPORT to determine first and second order parameters - in other words the basic layout of the system. RAYTRACE is then used to fine tune the system. First and second order parameters generally have to be readjusted slightly, and when dipoles are involved there are also zeroth order adjustments, i.e., centerline offsets. The major function of RAYTRACE however, is to calculate higher-order aberrations in the optics, and to be an aid in correcting these aberrations, whenever possible. The program, as described here, does not have a built-in automatic fitting routine for minimizing image aberrations, etc., but it has been used as a subroutine for such programs.^{2,3}

Since the program traces one ray at a time, it is not readily adaptable to handle space charge forces as they occur in systems with intense beams. Such forces can sometimes be mimicked by the introduction of strings of defocusing lenses. However, since the strengths of these lenses depend upon the beam diameter and vice versa the procedure is a lengthy cut-and-try one. A better program for such calculations is the Electron Trajectory Program developed by W. B. Hermannsfeldt.⁴

II. General Ion Optics

In discussing ion optical devices, we borrow the terminology from light optics. Words such as focussing, dispersion, focal lengths, principal planes, resolution, etc. all have the same meaning in ion optics as in light optics. A convex glass lens has the property that light rays passing through it are deflected towards the axis by an angle that to first order is proportional to the distance from the center of the lens. As a result, a bundle of parallel rays converges towards a point after passing the lens. Ion optical lenses, i.e. solenoids, quadrupoles and deflecting magnets, focus bundles of ions in much the same way, but with some additional complications. A solenoid twists the beam as it focuses, and a quadrupole or the fringing fields of a deflecting magnet act as a converging lens in one plane and a diverging lens in the perpendicular plane.

In order to describe what happens to a bundle of ion rays passing through one or more ion-optical devices, we introduce the concept of transfer coefficients. The box in Fig. 1 represents any ion-optical transfer system consisting of magnetic dipoles, electro-static deflectors, quadrupoles, solenoids, and higher order multipoles. A particle is assumed to be emitted from (or passing through) point x_1, y_1 in the plane $z_1 = 0$. After having traversed the system, it will be detected at position x_2, y_2 in the plane $z_2 = 0$. The direction of the particle before entering the system is specified by the angles θ and ϕ defined in the figure. A reference momentum p_0 is assumed, and the deviation from this momentum is given as $\delta = \Delta p/p_0$. For simplicity, we shall in the following discussion assume that the system is mechanically symmetric about the xz -plane and that for $y = 0$ the magnetic field is everywhere perpendicular to this symmetry plane. This then will have to be the median plane of any dipole magnet (deflecting magnet) and a symmetry plane between poles of any quadrupole or higher order multipole magnet. Solenoids violate this condition but can under certain circumstances be included if an appropriate rotation of the coordinate system is performed.

The ray position at the exit is clearly a function of the position and direction at the entrance and of the momentum. Thus,

$$x_2 = f(x_1, \theta_1, y_1, \phi_1, \delta) \quad (1)$$

with similar expression for θ_2, y_2 , and ϕ_2 . We now assume that the exit coordinate system has been placed such that a particle with momentum p_0 emitted along the x_1 axis exits along the x_2 axis. We can then express Eq. (1) as a Taylor expansion in $x_1, \theta_1, y_1, \phi_1$, and δ :

$$\begin{aligned} x_2 = & (x/x)x_1 + (x/\theta)\theta_1 + (x/\delta)\delta + (x/x^2)x_1^2 \\ & + (x/x\theta)x_1\theta_1 + (x/\theta^2)\theta_1^2 + (x/x\delta)x_1\delta \\ & + (x/\theta\delta)\theta_1\delta + (x/\delta^2)\delta^2 + (x/y^2)y_1^2 + (x/y\phi)y_1\phi_1 \\ & + (x/\phi^2)\phi_1^2 + \text{higher order terms} \end{aligned} \quad (2)$$

The factor (x/x) , called a transfer coefficient, is actually the first-order derivative $\partial x_2/\partial x_1$. Similarly, the term (x/θ) is equal to $\partial x_2/\partial \theta_1$, etc. The term (x/x) is the magnification of the system in the x direction and (x/δ) is the dispersion; it measures the displacement in the x direction at the exit per unit change in δ . Because of the assumed symmetry about the median plane, terms of the form $(x/y^n\phi^m)$ vanish unless the sum $n + m$ is even. Therefore, there is no term such as (x/ϕ) in Eq. (2).

RAYTRACE tracks one ray at a time through each element of the system using step by step numerical integration. If desired, a number of rays can be traced sequentially to determine transfer coefficients such as those in Eq. (2). If certain standard sets of rays are used, the evaluation of the coefficients, up to fifth order, is performed by routines that are part of the **RAYTRACE** package.

III. Raytracing

The motion of a particle carrying a charge Q is governed by the Lorentz force,

$$\vec{F} = Q[\vec{E} + \vec{v} \times \vec{B}], \quad (3)$$

where \vec{E} is the electric field and \vec{B} is the magnetic field. In a rectangular (x, y, z) coordinate system the equations of motion along each of the axes may be written as

$$\begin{aligned} d(m\dot{x})/dt &= Q(E_x + v_y B_z - v_z B_y) \\ d(m\dot{y})/dt &= Q(E_y + v_z B_x - v_x B_z) \\ d(m\dot{z})/dt &= Q(E_z + v_x B_y - v_y B_x) \end{aligned} \quad (4)$$

In **RAYTRACE** the equations of motion are solved by means of a step-by-step numerical integration with time as the independent variable. A fourth-order Runge-Kutta integration routine is used. When sufficiently small step sizes are taken, the accuracy is limited only by the uncertainties in our knowledge of the electric and magnetic fields. Round-off errors are negligible if the standard double-precision version of **RAYTRACE** is used. Various routines describe the field distribution in terms of a few simple parameters for each type of element. Most of these parameters are directly related to dimensions and specifications on an engineering drawing of the element. The modular nature of the code allows easy access for addition of new devices or modification of the 'field' routines to correspond to specific needs.

In most of the elements, the particle typically moves through three distinct regions: the entrance fringing field, the 'uniform' field and the exit fringing field. Figure 2 shows, as an example, the layout for a dipole magnet. The different coordinate systems are related by a non-real geometrical ray ABCD which is a straight line from A to B, a circular arc from B to C, and a straight line from C to D. All calculations are made with reference to the four rectangular coordinate systems with origins at A, B, C and D. The rest of the dipole parameters are discussed in detail in Sec. V.

Each element has an input coordinate system and an output coordinate system such as A and D for the DIPOLE. The output coordinate system of one element coincides with the input coordinate system of the next element. As presently written the code can handle 200 elements and trace 100 rays through them.

The program calculates the path of one particle at a time through all elements of the system. If desired, every step is printed out on a single line giving the independent variable, time (converted to path length into the system), position, velocity components, field components and the angles θ and ϕ indicating directions relative to the yz -plane and the xz -plane.

There are three options for a final coordinate system in which the positions and directions of the rays are given:

- a) the D-axis system of the final element
- b) z -axis along the projection of ray number 1 on the xz -plane, origin at $z_D = 0$
- c) z -axis as for case b but with origin where the projections (on the xz -plane) of ray 1 and ray 2 intersect.

Figure 3 shows the positions of three "focal axes" systems relative to the D coordinate system for the final element. The positions of the origins for different energies form a focal surface. For a spectrometer the detectors are placed on or near this focal surface.

A set of fourteen rays with specified initial angles θ and ϕ and all originating from the same point (the source) can be used to calculate transfer coefficients depending upon θ and ϕ only, from first to fifth order (e.g., $x/\theta^2\phi^2$). If the fourteen rays are run for five different energies, the program will calculate the focal plane angle and chromatic aberration coefficients such as $x/\theta^2\delta^3$, etc. Another option is to use a specified set of 46 rays to calculate first, second and third order coefficients for x, θ, y , and ϕ at the exit in terms of x, θ, y, ϕ at the entrance and $\delta = \Delta p/p$.

The units used in **RAYTRACE** are:

lengths:	cm
angles, general:	degrees
beam direction:	milliradians
energy:	MeV
magnetic fields:	Tesla
electric fields:	kV/cm

IV. General Routines

All of the routines used in **RAYTRACE** are coded in **FORTRAN** and are intended to be computer independent. Most of the subroutines are element specific and will be discussed separately in Sec. V. The routines that do not fall in this category are the following:

A. MAIN.

This main routine handles the data flow including the input and output.

B. RAYS.

This subroutine is used to generate standard sets of rays that are used in calculating first and higher-order transfer coefficients. There are four sets with 2, 6, 14, and 46 rays. The four sets are generated using specifications in a single record immediately following the **SENTINEL** terminator.

The two-ray set generates a central ray with x, y, θ , and ϕ all zero and a second ray with specified θ and ϕ such that the first order transfer coefficients x/θ , θ/θ , y/ϕ , and ϕ/ϕ can be determined.

The six-ray set generates five evenly spaced rays in θ -space plus a paraxial ray used to locate the first-order image position. From this set aberrations of the form x/θ^n can be determined up to $n = 5$.

The fourteen-ray set is used to generate 8 off-median plane rays in addition to the six rays mentioned above. Aberrations of the form $x/\theta^n \phi^m$ can be determined up to $n + m = 5$. Similarly, aberrations in the coordinates θ, y , and ϕ can be determined.

Finally, the forty-six-ray option generates a set from which aberration coefficients depending upon x, θ, y, ϕ , and δ are calculated.

Any number of individual rays can be entered following the single record discussed above — as long as the number of rays to be calculated does not exceed 100.

C. OPTIC.

This subroutine deals with the output rays following the last element in the system. Specifically, it calculates the intersection between each ray and Ray 1 (presumably the central ray). Depending upon the value of **JFOCAL** (0, 1, or 2) it prepares the rays for printout in one of three coordinate system:

JFOCAL = 0 — Intersection of Rays 1 and 2 or, actually, their projections on the xz -plane defines a new origin. Ray 1 or its projection defines a new z -axis. All rays are printed out in this "Optic Axis System." (Fig. 3.)

JFOCAL = 1 — Ray 1 or its projection forms a new z -axis, but the origin is at the intersection between Ray 1 or its projection with the xy -plane of the D -axis system of the last element.

JFOCAL = 2 — The rays are printed out in the D -axis system of the last element.

D. PRNT.

Controls the printing of all input and output data.

E. MATRIX.

This subroutine calculates transfer coefficients for the case where a standard set of 46 rays have been traced. First and second order coefficients are printed out as matrices in exactly the same format as used in the ion-optics program **TRANSPORT**. Some of the higher-order coefficients are then listed separately. A sample output is shown in Appendix 4.

F. MTRX1.

This subroutine calculates transfer coefficients for the 6-ray and the 14-ray options. In both cases a point source is assumed. For each energy a list of coefficients is computed. The coefficients are printed out in units of cm and milliradians and separately in meters and radians. In the latter case it is equivalent to

the "non-dimensional" units sometimes used in the literature for spectrometers if the layout radius for the dipoles happens to be $R=1$ m. At the bottom of the list of transfer coefficients are several entries with a label "trunc" attached. These are combinations of two coefficients, for instance x/θ^2 and x/θ^4 . They are coefficients that would have resulted if the power series formed by the coefficients had been truncated at third- rather than fifth-order.

At the top of the list MTRX1 presents the kinetic energy, the coordinates x and z for the origin of the optic axis system relative to the final D-axis system, the orientation θ of the z -axis, the total width of the "image" in x and y , the x -waist of the beam and the position of the waist.

When MTRX1 is used, the last page of the printout is a summary table of the transfer coefficients for all energies in units of meters and radians. If five energies are run, there will also be, at the bottom of the page a printout of the focal-plane angle and energy-dependant coefficients such as $x/\theta\delta^2$, representing the second order curvature of the focal surface, and $x/\theta^2\delta$, etc. A sample output is shown in Appendix 4.

G. DERIV.

This subroutine combines velocities and fields to present the equations of motion to be solved.

H. FNMIRK.

This is the Runge-Kutta integration routine used to solve the equations of motion.

I. PLTOUT.

This routine stores step-by-step position information for each ray to be used by plotting routines such as RAYGRAPH.

V. Element Routines

A. DIPOLE. Magnetic Dipole.

The dipole subroutine requires 12 records in the input data file. A short description of these records is given in Appendix 1. A more detailed description of the subroutine is presented here. However, it is necessary first to discuss in some detail the meaning of the term "the effective field boundary" (EFB).

Fig. 4 shows a set of pole profiles with coil cross section used in a modern dipole (for a spectrometer). The 30- and 75-degree cuts produce a crude approximation to a Rogowski profile.⁵ The three examples show a "regular" profile, a profile with "field clamp" (magnetic short-circuit), and one with a removable insert used to adjust the position of the "Effective Field Boundary" (EFB). The dash-dotted lines indicate the positions of the EFB, defined as the position of sharp cutoff of the field with the same field integral as the real distribution assuming the integration is performed along a straight line. Two practical questions need to be discussed:

1. What is the meaning of the term effective field boundary for a charged particle which moves along a curved path?
2. What is the position of the effective field boundary if the mechanical boundary has a curvature?

As far as **RAYTRACE** is concerned the first question can be dismissed immediately as irrelevant. The program needs a prescription for calculating the field at a given point in the fringing field region, given some pole profile and given some curvature of the mechanical pole boundary projected on the xz -plane.

The second question is more difficult to answer, especially if the curvature called for is not a simple circular one, concave or convex. The problem has been resolved by redefining the EFB as a mechanical reference boundary – a curve following the mechanical shape of the pole piece. The position of the EFB, relative to the pole piece is the position calculated on the assumption that the boundary is straight. With tapered poles such as shown in Fig. 4, the taper should preferably be of such a depth that the EFB coincides with the contour at the root of the pole. This makes the engineering design and installation much easier and less prone to errors.

1) MTYP=1 (Homogenous Field): General Description

The **DIPOLE** subroutine has 6 options identified with a parameter called **MTYP** with values 1 through 6. The data records are very similar for all six and the particle tracking through the magnet is similar for all. The difference lies in the field descriptions, both in the fringing and "uniform" fields. The following general description applies to a homogenous field magnet (**MTYP**=1) with the simplest treatment of the fringing field. The differences between the **MTYP**'s are then described in subsequent sections.

The general layout of a magnetic dipole is shown in Fig. 2 where the most important parameters are defined. The input coordinate and velocity components of a particle are given in coordinate system A. The first step is to make a transformation to system B.

$$\begin{aligned}x_B &= (A - z_A) \sin \alpha - (x_A + \text{XCR1}) \cos \alpha \\y_B &= y_A \\z_B &= (A - z_A) \cos \alpha + (x_A + \text{XCR1}) \sin \alpha \\(v_x)_B &= -(v_x)_A \sin \alpha - (v_z)_A \cos \alpha \\(v_y)_B &= +(v_y)_A \\(v_z)_B &= -(v_z)_A \cos \alpha + (v_x)_A \sin \alpha\end{aligned}\tag{5}$$

The constant **XCR1** appears in Fig. 2. Its significance is discussed later. The particle is next carried along a straight line to the beginning of the entrance fringing field as defined by the parameter **Z11**. Note that the "object distance" **A** can be zero or even negative. The "image distance" **B** of one element and the "object

distance" A for the next must, of course, add up to the physical distance between the elements. How this distance is divided is dictated by where the user wants to see an intermediate printout.

Consider first a particle moving in the median plane. The particle is carried through the entrance fringing field zone by numerical integration of the equations of motion with a magnetic field given by

$$B_y = \frac{B_0 - B_R}{1 + e^s} + B_R \quad (6)$$

on the median plane. B_0 is the uniform field (MTYP=1) inside the gap of the magnet, B_R is the asymptotic constant field outside the magnet (normally 0) and S is a parameter that increases monotonically with z (in the B -axis system). It is expressed as a power series in the parameter s :

$$S = C00 + C01s + C02s^2 + C03s^3 + C04s^4 + C05s^5. \quad (7)$$

For a straight-line effective field boundary (EFB) we have

$$s = z/D \quad (8)$$

where D is the magnet airgap. Equation (6) gives the correct asymptotic behavior of the field for $z \rightarrow \pm\infty$ provided C05 is positive. The basic integration step size in the entrance fringing field is LF1 which is an input parameter (Appendix 1). The recommended value is LF1= 0.3D or smaller.

The coefficients in Eq. (7) are generally determined by a least-square fit between the field given by Eqs. (6,7,8) and either a measured field or a field calculated by the aid of programs such as POISSON⁶. We generally find that the exact shape of the fringing field curve is not so important for the optical properties of a dipole, provided the coefficients used produce an effective-field boundary at $z = 0$ and approximately the correct slope for the curve B vs. z . For details see reference 7.

If the EFB is curved, a correction $\Delta s = \Delta z/D$ is made to Eq. (7) with Δz given by

$$\Delta z/R = -[S02(x/R)^2 + S03(x/R)^3 + \dots + S08(x/R)^8] \quad (9)$$

Here R is the layout radius for the dipole and the $S0n$'s are coefficients describing curvatures of 2nd and 3rd orders, etc. This simple correction ($\Delta s = \Delta z/D$) applies to MTYP=1 only.

If the curvature of the EFB is circular one can instead of the $S0n$'s read in a parameter RAP1 (RAP2 for the exit) which is the inverse of the radius of curvature in cm^{-1} . The program will then convert RAP1 to a power series in (x/R) with even order terms up to eight order. If the data also contains non-zero parameters S02, etc. these will be added to those calculated from RAP1 (RAP2). RAP1 and RAP2 are positive for convex boundaries.

The program continuously tests if the particle has passed the plane $z = -Z12$. If it has passed it on a given step, it is brought back to the previous point and carried forward with a reduced step size such that it lands approximately on the plane. The coordinates are then transformed to system C at the exit effective edge.

$$\begin{aligned} x_C &= -z_B \sin(\varphi - \alpha - \beta) - x_B \cos(\varphi - \alpha - \beta) - 2R \sin \frac{\varphi}{2} \sin(\frac{\varphi}{2} - \beta) \\ y_C &= y_B \\ z_C &= -z_B \cos(\varphi - \alpha - \beta) + x_B \sin(\varphi - \alpha - \beta) - 2R \sin \frac{\varphi}{2} \cos(\frac{\varphi}{2} - \beta) \\ (v_x)_C &= -(v_x)_B \sin(\varphi - \alpha - \beta) - (v_y)_B \cos(\varphi - \alpha - \beta) \\ (v_y)_C &= (v_y)_B \\ (v_z)_C &= -(v_z)_B \cos(\varphi - \alpha - \beta) + (v_x)_B \sin(\varphi - \alpha - \beta) \end{aligned} \quad (10)$$

The integration through the uniform part of the field is straightforward with $B_y = B_0$. Again, the program continuously tests if the particle has passed the plane $z = Z21$, and a correction is made such that it lands approximately on the plane. It is then carried through the exit fringing field where the field description is identical to that of the entrance fringing field with the appropriate parameters. After the particle has been deposited approximately on the plane $z = Z22$ a coordinate transformation is made to system D.

$$\begin{aligned}
x_D &= z_C \sin \beta + x_C \cos \beta - XCR2 \\
y_D &= y_C \\
z_D &= z_C \cos \beta - x_C \sin \beta - B \\
(v_x)_D &= (v_x)_C \sin \beta + (v_z)_C \cos \beta \\
(v_y)_D &= (v_y)_C \\
(v_z)_D &= (v_z)_C \cos \beta - (v_x)_C \sin \beta
\end{aligned} \tag{11}$$

The particle is then translated along a straight line until it intersects with the xy -plane ($z_D = 0$) of that system.

If the path length of a particle inside the dipole is relatively short, it may never be in anything close to a uniform field. The recommendation is then *not* to reduce the absolute values of Z12 and Z21 but to let the two fringing field zones overlap. The program then integrates the equations of motion *backwards* through the uniform field. Fig. 5 illustrates the effect of this procedure. The total field integral corresponds to the area under the partially dashed curve in Fig. 5. The result is essentially that in the middle the deficiencies for both curves are added to a total deficiency as shown. This procedure simplifies the work for the designer. He doesn't have to worry about overlap, wholly or partially by the fringing field zones. One warning is in order, though: the particle orbit must intersect the beginning of the exit fringing field zone either by moving forward or backwards; otherwise, it will start moving in circles in a uniform field. The program cuts off the integration after 200 steps in either zone and prints out the message: "Exceeded maximum number of steps in element i , zone j ".

For particles moving off the median plane the formula for the component B_y is modified and the components B_x and B_z are also evaluated. This is done by Taylor expansions in y through third order for B_x and B_z and through fourth order for B_y . Symmetry about the median plane insures that B_x and B_z contain only odd orders of y and B_y only even orders. The corresponding expressions are

$$\begin{aligned}
B_x &= (y/1!) \partial B_x / \partial y + (y^3/3!) \partial^3 B_x / \partial y^3 \\
B_y &= B_y + (y^2/2!) \partial^2 B_y / \partial y^2 + (y^4/4!) \partial^4 B_y / \partial y^4 \\
B_z &= (y/1!) \partial B_z / \partial y + (y^3/3!) \partial^3 B_z / \partial y^3
\end{aligned} \tag{12}$$

where the fields and their derivatives on the right hand side are to be evaluated at $y = 0$.

The derivatives appearing in these equations are all computed by the use of Maxwell's equations converting derivatives of the kind $(\partial^{i+j} B_y / \partial x^i \partial z^j)_{y=0}$ into the desired forms. The derivatives of B_y in the median plane are determined numerically by calculating $(B_y)_{y=0}$ in a thirteen-point grid. Figure 6 shows such a grid. The grid constant DG is an input parameter (see Appendix 1) which should be given a value of the order of $0.3D$. The results of the Taylor expansions (with $\Delta = DG$) are

$$\begin{aligned}
B_y &= B_{00} - \frac{y^2}{\Delta^2} \left[\frac{2}{3} (B_{10} + B_{-10} + B_{01} + B_{0-1} - 4B_{00}) - \frac{1}{24} (B_{20} + B_{-20} + B_{02} + B_{0-2} - 4B_{00}) \right] \\
&+ \frac{y^4}{\Delta^4} \left[-\frac{1}{6} (B_{10} + B_{-10} + B_{01} + B_{0-1} - 4B_{00}) + \frac{1}{24} (B_{20} + B_{-20} + B_{02} + B_{0-2} - 4B_{00}) \right. \\
&\left. + \frac{1}{12} (B_{11} + B_{-11} + B_{1-1} + B_{-1-1} - 2B_{10} - 2B_{-10} - 2B_{01} - 2B_{0-1} + 4B_{00}) \right]
\end{aligned} \tag{13}$$

$$B_x = \frac{y}{\Delta} \left[\frac{2}{3}(B_{10} - B_{-10}) - \frac{1}{12}(B_{20} - B_{-20}) \right] + \frac{y^3}{\Delta^3} \left[\frac{1}{6}(B_{10} - B_{-10}) - \frac{1}{12}(B_{20} - B_{-20}) - \frac{1}{12}(B_{11} + B_{1-1} - B_{-11} - B_{-1-1} - 2B_{10} + 2B_{-10}) \right] \quad (14)$$

$$B_x = \frac{y}{\Delta} \left[\frac{2}{3}(B_{01} - B_{0-1}) - \frac{1}{12}(B_{02} - B_{0-2}) \right] + \frac{y^3}{\Delta^3} \left[\frac{1}{6}(B_{01} - B_{0-1}) - \frac{1}{12}(B_{02} - B_{0-2}) - \frac{1}{12}(B_{11} + B_{-11} - B_{1-1} - B_{-1-1} - 2B_{01} + 2B_{0-1}) \right] \quad (15)$$

where the subscripts refer to the index number of the points in Fig. 6.

For an MTYP=1 magnet the coefficients describing the variation of B_y vs. radial position: n, BET1, GAMA and DELT (Appendix 1) are zero. If the data record for these constants have non-zero values these values are ignored.

In the input data there appear four more constants that need explanation. The first two are XCR1 and XCR2, both of which are identified in Fig. 2. The layout ray for the dipole connecting the origins of the four coordinate systems is a non-real ray consisting of a straight line, a circular arc and another straight line. No real particle will follow this trajectory. If one somewhat arbitrarily, insists that a ray defined as the central ray shall follow the layout circular arc inside the magnet - and therefore have a magnetic rigidity of $B_0 R$ - corrections must be made outside. That is, one must shift the magnet relative to the centerline of other optical elements by an amount⁷

$$XCR1 = D^2 I_1 / R \cos^2 \alpha \quad (16)$$

where I_1 is an integral that depends upon the shape of the fringing field. It may vary from $I_1 = 0.3$ for a "short-tail" fringing field to about $I_1 = 0.7$ for a "long-tail" fringing field. The shift at the exit is similar with α replaced by β . For a symmetric magnet ($\alpha = \beta$) the shifts may not be necessary in practice. A particle moving along the z_A axis can be made to exit along the z_D axis by adjustment of the magnetic field. It will then move on an inside track relative to the layout arc inside the magnet. The corrections discussed here are a nuisance for the engineer who is laying out the system and should not be used unless they are important. Whether or not they are used, RAYTRACE will always predict the correct positions and angles of the rays traced.

The two remaining dipole parameters are DELS1 and DELS2. These can be used to shift the positions of the effective field boundaries at entrance and exit, respectively. For instance, if field mapping indicates that the EFB at entrance is off by an amount Z_{err} into the magnet from its intended position, RAYTRACE can be re-run with

$$DELS1 = Z_{err} / D \quad (17)$$

In general, Eq. (8) now becomes (for MTYP=1)

$$s = (z + \Delta z) / D + DELS1 \quad (8a)$$

Of course, DELS2 serves a similar purpose at the exit of the dipole.

In the past DELS1 has been used to correct for the position of the effective field boundary due to the curvature of the boundary. The effective field boundary for a magnet with convex curvature is closer to the magnet than when the boundary is straight - assuming the same pole piece profile. If the same coefficients C00-C05 are used to describe the fringing field for both cases, DELS can be used to correct the position of the EFB, but of course not the shape of the $B_y(z)$ curve.⁸ In the current version for MTYP=2, we attempt to make the correction due to curvature in a more direct way, applicable to a boundary of any shape (within reason) and without the use of DELS.

A new feature has been added to the dipole routines, MTYP=1...5. The field distribution on the median plane of the fringing field can be precalculated and stored in an array with a distance DG between neighbouring points. When a ray is traced through the fringing field zone, the field on the median plane for a given point is determined by interpolating between neighbouring grid points. If the particle is not in the median plane, the interpolation routine must be used thirteen times and the field components calculated as described earlier (Eqs. 13-15).

This new feature can result in a considerable saving in computer time when a large number of rays are to be traced or when the system contains a number of identical dipoles. The feature is activated by specifying an array number IMAP for the dipole (see Appendix 1). Identical dipoles would have the same value for IMAP ≤ 5 .

The array on the entrance side will have $n_x \cdot n_z$ points where

$$\begin{aligned} n_x &= (WDE + 2Z11 \tan \alpha) / DG + 6 \\ n_z &= (Z11 - Z12) / DG + 6. \end{aligned}$$

Corresponding expressions apply to the exit side.

2) MTYP=2. Homogenous-Field Dipole

The only difference between MTYP=1 and MTYP=2 is the way the parameter s is calculated. In both cases s represents distances to the effective field boundary. In MTYP=1 sD is simply the distance to the EFB measured in the z -direction, i.e. not generally the shortest distance. In MTYP=2 the shortest distance to the effective field boundary from a given point is determined. However, this is not simply used to calculate s as distance/ D . Rather, the line representing the shortest distance is only the middle one of a spray of 5 lines from the point the particle is at. An average, strongly weighted towards the middle line, is then used to calculate a representative distance and thereby s . The averaging is weighted in such a way that if the boundary is straight, sD is exactly equal to the shortest distance.

Assume first that the shortest distance from point P to the EFB has been found. This distance, r_3 in Fig. 7, is divided by four, and the distances to four other points 1,2,4, and 5 are determined with the relationship between the x -coordinates for the points being (see Fig. 7):

$$x_{i+1} = x_i + \frac{r_3}{4} \cos \theta_3 \quad (18)$$

The formula used to calculate s is

$$sD = 1.41875 \left(\sum_{i=1}^5 r_i^{-4} \right)^{-1/4} \quad (19)$$

The algorithm for finding the shortest distance is as follows:

- a) The distance in the z -direction from point P to the EFB is determined as for MTYP=1.
- b) This distance is compared to the distance from point P to the origin. The shortest of the two, call it a , is divided by 5.
- c) The square of the distance from point P to 11 points on the EFB is calculated, 5 points on each side of point A (Fig. 7) in addition to $(z_P - z_A)^2$. Between two neighbouring points the distance in the x -direction is $\Delta x = a/5$.
- d) The 11 distances squared are compared and the smallest of these is selected.

- e) The x -distance between the two points on either side of the selected shortest distance is further subdivided by 10 to $\Delta x = a/25$, and squares of distances are calculated between the field point P and the points on the field boundary.
- f) Again the smallest of the 11 squares and its smallest neighbour are selected. Call the distance to the point with the lowest x -value r_1 and call the other r_2 .
- g) Another subdivision is now performed to find an even shorter distance, but this time by the use of some trigonometry (see Fig. 8). It is assumed that the EFB between the two points (with $\Delta x = a/25$) can be considered to be a straight line. This is line c , the length of which is grossly exaggerated compared to r_1 and r_2 in Fig. 8. Some elementary trigonometry applied to the triangles in Fig. 8 yields

$$x_3 = x_1 + \frac{c^2 + r_1^2 - r_2^2}{2c^2}(x_2 - x_1) \quad (20)$$

This then determines the central point on the EFB for the spray of five lines, discussed above.

As explained earlier for MTYP=1 when the particle is off the median plane the field B_y in the median plane must be determined 13 times such that the appropriate derivatives can be calculated. The relative accuracy of these determinations of B_y -values has to be high, especially if y/DG is much larger than unity (see Eq. 13).

We call the representative distance for the central point $s_0 D$. The corresponding values for the other twelve points are then determined as

$$sD = s_0 D + \Delta sD \quad (21)$$

where ΔsD is given by (see Fig. 9)

$$\Delta sD = s_0 D + DG(i \cos \delta - j \sin \delta) - (z_{x_1} - z_P + A \sin \delta) \cos \delta \quad (22)$$

with

$$A = DG(j \cos \delta + i \sin \delta), \quad (23)$$

$$x_1 = x_P + A \cos \delta$$

and

$$\delta = \arctan(dz/dx) \quad (24)$$

at the point P. The two indices i and j identify the grid point. They are the numbers appearing in Fig. 6.

Since the Runge-Kutta integration routine looks up the field components B_x , B_y , and B_z four times for each integration step, altogether 52 values of sD have to be determined for each integration step.

The program, of course, determines if the integration point is inside or outside the EFB. With any reasonable boundary corresponding to a practical magnet, the computer should have no trouble in finding the shortest distance to the boundary. It is, however, possible for the ion-optical designer to confuse the computer with indiscriminate use of higher order corrections. Figure 10 shows an example that speaks for itself. It is generally wise to use eighth order terms S08 and S18 to represent the limited width of the pole pieces. For instance, if the pole width is W as measured in the x -direction an eighth-order correction term $S08 = 50DR^7/W^8$ will push the EFB towards the corner of the pole piece by an amount $-\Delta z = 0.2D$ at $x = \pm W/2$. This is the right order of magnitude.

3) MTYP=3. Dipole with Field Gradient.

MTYP=3 is used for a dipole with nonzero value for any of the parameters n , BET1, GAMA, or DELT. This includes otherwise uniform-field magnets for which one wishes to study the effect of limited pole face

width. The fourth order term DELT is then probably the most appropriate term to use. The field description on the median plane in the "uniform" region for MTYP=3 is

$$B_y = B_0[1 - n\Delta r/R + \text{BET1}(\Delta r/R)^2 + \text{GAMA}(\Delta r/R)^3 + \text{DELT}(\Delta r/R)^4] \quad (25)$$

and the field off the median plane is determined by a Taylor expansion in y using analytic derivatives.

In the fringing-field region the method of determining the distance to the EFB is the same as in MTYP=2. The algorithm for determining B_y on the median plane depends upon whether the field point is inside or outside the EFB. Inside the EFB Eq. (25) is modified by the factor $(1 + e^S)^{-1}$. Outside the EFB the algorithm is further modified in the following way. A line is drawn parallel to the z -axis from the field point to its intersection with the EFB. This point of intersection is used to determine an artificial Δr_{EFB} which is used in the modified Eq. (25). The justification for this procedure is that it is assumed that outside the EFB the field distribution no longer senses the curvature radius R as it does inside the gap.

4) MTYP=4. Dipole with Field Gradient.

This subroutine is similar to MTYP=3 but with the following modification: The field description has been changed in such a way that with a single parameter, n , one can describe the field in a magnet with strictly conical pole faces, i.e.

$$B_y = B_0(1 + n\Delta r/R)^{-1} \quad (26)$$

The real reason why this subroutine was written was the need for describing a magnet with plane pole faces set at an angle to each other to form a wedge-shaped gap (The CLAMSHELL Spectrometer). Changing a conical surface to a plane surface is accomplished by making R very large and the layout deflecting angle φ very small. The layout path inside the gap is then approximately a straight line. In order for the particles to enter at an angle to this layout orbit, a coordinate rotation is executed at the entrance point and again at the exit point (Subroutine SHRT).

5) MTYP=5. Circular-Pole Dipole

This routine is designed for use with dipoles that have circular pole pieces, in particular superconducting magnets for which the pole piece is in saturation and there is no real uniform field region (Fig. 11). The effective field boundaries are circles with radius $R_m^{-1} = \text{RAP1} = \text{RAP2}$. The layout radius R should be made large and the angle φ small such that $R\varphi = 2R_M$. The entrance and exit angles are $\alpha = \beta = 0$ and the fringing-field zones are touching in the middle of the magnet, i.e., $Z_{12} = Z_{21} = -R_M$. The central ray can be directed into this magnet at any point and in any direction by using the element SHRT. Similarly, at the exit, the central ray can be made to follow the centerline of the next element by use of SHRT. If both centerlines intersect at the center of the circle, the simplest procedure is to place coordinate system D at the center and make a rotation about the y -axis there.

6) MTYP=6. Pretzel Magnet

The Pretzel magnet is often used to produce a net non-dispersive 90-degree bend⁹ of the electron beam from certain linear accelerators. The field description both on and off the midplane is:

$$\begin{aligned} B_x &= 0 \\ B_y &= \frac{B_0}{D} |z|^n \left[1 - \frac{1}{2} n(n-1) \left(\frac{y^2}{z^2} \right) + \frac{1}{24} n(n-1)(n-2)(n-3) \left(\frac{y^4}{z^4} \right) \right] \\ B_z &= \frac{B_0}{D} |z|^n \left[n \left(\frac{y}{z} \right) - \frac{1}{6} n(n-1)(n-2) \left(\frac{y^3}{z^3} \right) \right] \end{aligned} \quad (27)$$

which for $n = 1$ describes the field in half a quadrupole with a mirror plate at $z = 0$. Non-dispersive 270-degree deflection requires $n = 0.8$, $\phi = 270^\circ$, $\alpha = 45^\circ$, and $\beta = 45^\circ$. The beam then makes a loop in the

magnet and exits at the point of entrance (Fig. 12). In practice this of course requires a hole in the mirror plate.

Since for $n \leq 1$ B_z diverges as z approaches zero, a narrow "fringing" field zone is used for small values of $|z|$. In this zone n is made equal to unity (by the program). The width of the zone is set by the parameter DG (negative) which in this subroutine does not have the conventional meaning. For $z > 0$:

$$B_x = B_y = B_z = 0$$

The Pretzel magnet is also suitable for a very broad range spectrometer in which the detector is approximately along the symmetry line of the Pretzel, i.e. after 135-degree deflection. The dispersion here is approximately proportional to $\rho^{1/2}$ for $n = 1$. It is therefore possible to obtain a momentum range as large as 100 to 1.

B. EDIPL. Electrostatic Cylinder Deflector

The layout of the coordinate systems, input parameters, and computational techniques for the Electrostatic Deflector (Fig. 13) are very similar to those for the magnetic dipole. However, as mentioned in Sec. III, the integration of the equations of motion will produce changes in the kinetic energy of the ion as it moves through the electric field. Relativistic dynamics are used and the input data must include the mass and the charge of the particle (Record 3).

The data include the layout radius (mean radius) of the deflector, the angle of deflection – including deflection in the fringing field – the airgap, and the electric field. In the “uniform” region the electric field is described in coordinate system C by:

$$\begin{aligned} E_r &= -E_0 \frac{R}{r} \\ E_x &= E_r \cos \gamma \\ E_z &= E_r \sin \gamma \end{aligned} \quad (28)$$

where γ is defined by

$$\tan \gamma = -z/(R + x) \quad (29)$$

and where R is the layout radius and r is the distance from the center to the particle (Fig. 11).

The fringing-field description is similar to that for the magnetic dipole, particularly MTYP=3, but with some modifications. It is assumed that the lengths of the two electrodes are adjusted such that the distance to the EFB is the same for both electrodes. For positive z the field on the yz -plane ($y = 0$) is assumed not to sense the curvature radius R , but simply obey the equation

$$E_x = \mp \frac{E_0}{1 + e^S} \quad (30)$$

The negative sign applies for the entrance field and the positive sign for the exit field. The parameter S is given by Eq. (7) as for the magnetic dipole. A finite width of the electrodes in the y -direction is accounted for by writing

$$s = z/D + EC2(z/D + 1)y^2/W^2 + EC4y^4/W^4 \quad (31)$$

For negative values of z the field on the yz -plane has a component in the z -direction in addition to E_x . Equation (30) is then replaced by

$$E_x = \mp \frac{E_0}{1 + e^S} \cos^2 \gamma \quad (32)$$

$$E_z = \frac{E_0}{1 + e^S} \cos \gamma \sin \gamma \quad (33)$$

where γ is now defined by

$$\tan \gamma = -z/R. \quad (34)$$

Off the yz -plane the field components are calculated by use of Taylor expansions in x similar to the approach for the magnetic dipole. However, since the field (for $z < 0$) is not perpendicular to the yz -plane, it is necessary to include all terms in the expansions, which are carried to fourth order.

The zeroth-order offset of the beam in the two fringing fields, discussed for the magnetic dipole under section V.A.1, occurs also for the electrostatic dipole. Here it is also usually more important that the beam follows the central layout orbit because in most cases the gap D is kept to a minimum. It is advisable in practice, and therefore in the calculations to offset the central rays at entrance and exit by an amount:

$$\Delta x = D^2 I_1 / R \quad (35)$$

For the electrostatic deflector these offsets have to be made by the element SHRT. The specified offset should be negative at the entrance and positive at the exit.

The integral I_1 depends upon the thickness and rounding of the electrode ends. For lack of better data use $I_1 = 0.35$.

The electrostatic dipole has three integration zones. Particle tracking starts by transforming the initial coordinates to system B at the entrance effective edge.

$$\begin{aligned}
 x_B &= -x_A \\
 y_B &= +y_A \\
 z_B &= A - z_A \\
 (v_x)_B &= -(v_x)_A \\
 (v_y)_B &= +(v_y)_A \\
 (v_z)_B &= -(v_z)_A
 \end{aligned} \tag{36}$$

The particle is then translated along a straight line to the start of the entrance fringing field zone at $z = Z11$. The particle differential equations of motion are integrated through the fringing field region to the end of the zone at $z = Z12$.

Particle coordinates are then transformed to system C located at the exit effective edge.

$$\begin{aligned}
 x_C &= -z_B \sin \varphi - x_B \cos \varphi - 2R \sin^2 \varphi / 2 \\
 y_C &= y_B \\
 z_C &= -z_B \cos \varphi + x_B \sin \varphi - 2R(\sin \varphi / 2) \cos \varphi / 2 \\
 (v_x)_C &= -(v_x)_B \sin \varphi - (v_z)_B \cos \varphi \\
 (v_y)_C &= (v_y)_B \\
 (v_z)_C &= -(v_z)_B \cos \varphi + (v_x)_B \sin \varphi
 \end{aligned} \tag{37}$$

The particle differential equations of motion are integrated through the "uniform" field to the start of the exit fringing field zone at $z = Z21$. Subsequently the particle is tracked through the fringing field region to the end of the zone at $z = Z22$.

Particle coordinates are then transformed to the output system D.

$$z_D = z_C - B \tag{38}$$

All other coordinates and the velocity components remain unchanged. Finally, the particle is translated along a straight line to the intersection with the plane $z_D = 0$, of system D.

C. POLES. Multipole (Quadrupole, etc.)

This subroutine is used for tracing rays through a quadrupole, sextupole (hexapole), octupole, decapole, dodecapole or a multipole with any mixture of these multipole components. Fig. 14 shows as an example a quadrupole with fairly strong higher-order corrections¹⁰ used in a spectrometer system. The calculation technique used in POLES is very similar to that used in a dipole: Four coordinate systems are used and the integration proceeds through an entrance fringing field zone, a "uniform zone" which means uniform field derivatives, and an exit fringing field zone. In the uniform zone the field is expressed as the gradient of

$$\phi = \sum_{n=1}^5 (n+1)^{-1} B_n R^{-n} r^{n+1} \sin(n+1)\theta \quad (39)$$

where B_n is the value of the field of the $2(n+1)$ -pole contribution at the aperture radius R .

The corresponding gradients, G_n , are given by

$$G_n = \frac{B_n}{R^n} \quad (40)$$

The field components in the uniform zone are then given by

$$\begin{aligned} B_x &= G_1 y + G_2 (2xy) + G_3 (3x^2 y - y^3) + G_4 (x^3 y - xy^3) + G_5 (5x^4 y - 10x^2 y^3 + y^5) \\ B_y &= G_1 x + G_2 (x^2 - y^2) + G_3 (x^3 - 3xy^2) + G_4 (x^4 - 6x^2 y^2 + y^4) + G_5 (x^5 - 10x^3 y^2 + 5xy^4) \\ B_z &= 0 \end{aligned} \quad (41)$$

In the fringing fields the gradients of the fields along the axis are multiplied by the functions

$$G_n^{(0)} = G_n / (1 + e^S) \quad (42)$$

with:

$$S = C00 + C01s + C02s^2 + C03s^3 + C04s^4 + C05s^5 \quad (43)$$

and

$$s = z/R \quad (44)$$

Just like in the dipole, z is measured from the effective field (gradient) boundaries. The length of the element L determines the position of the effective field boundaries for the quadrupole term (Fig. 15). The higher-order terms may have slightly different positions for the EFB. This is allowed for by use of the input parameters DSH, DSO, DSD and DSDD which displace the respective EFB's inward (if positive). For instance $\Delta z = \text{DSH} \times R$ for the sextupole. There are, finally also a set of parameters to allow for a faster (or slower) falloff of the fringing-field gradients for the higher-order components. The input parameters are FRH, FRO, FRD, and FRDD. If FRH=0.9 for instance the falloff of the sextupole gradient is the same as if the radius were equal to 0.9R, i.e. faster.

Off axis the field in the multipole is calculated by Taylor expansions from the axis. The derivatives are calculated analytically in this case and carried to at least fifth order in x and y .

In Eqs. (46-51) we summarize the formulas for the field components due to each of the multipole contributions. In these expansions the symbol $G_n^{(i)}$ represents the i th derivative with respect to s of the gradient $G_n^{(0)}(s)$.

$$\begin{aligned} G_n^{(1)} &= \frac{dG_n^{(0)}}{ds} \\ G_n^{(2)} &= \frac{d^2 G_n^{(0)}}{ds^2}, \text{ etc.} \end{aligned} \quad (45)$$

Quadrupole ($n = 1$):

$$\begin{aligned}
B_{1x} &= G_1^{(0)}y - \frac{1}{12}G_1^{(2)}(3x^2y + y^3) + \frac{1}{384}G_1^{(4)}(5x^4y + 6x^2y^3 + y^5) \\
&\quad - \frac{1}{23040}G_1^{(6)}(7x^6y + 15x^4y^3 + 9x^2y^5 + y^7) \\
B_{1y} &= G_1^{(0)}x - \frac{1}{12}G_1^{(2)}(x^3 + 3xy^2) + \frac{1}{384}G_1^{(4)}(x^5 + 6x^3y^2 + 5xy^4) \\
&\quad - \frac{1}{23040}G_1^{(6)}(x^7 + 9x^5y^2 + 15x^3y^4 + 7xy^6) \\
B_{1z} &= G_1^{(1)}xy - \frac{1}{12}G_1^{(3)}(x^3y + xy^3) + \frac{1}{384}G_1^{(5)}(x^5y + 2x^3y^3 + xy^5)
\end{aligned} \tag{46}$$

Hexapole ($n = 2$):

$$\begin{aligned}
B_{2x} &= G_2^{(0)}(2xy) - \frac{1}{48}G_2^{(2)}(12x^3y + 4xy^3) \\
B_{2y} &= G_2^{(0)}(x^2 - y^2) - \frac{1}{48}G_2^{(2)}(3x^4 + 6x^2y^2 - 5y^4) \\
B_{2z} &= G_2^{(1)}(x^2y - y^3/3) - \frac{1}{48}G_2^{(3)}(3x^4y + 2x^2y^3 - y^5)
\end{aligned} \tag{47}$$

Octupole ($n = 3$):

$$\begin{aligned}
B_{3x} &= G_3^{(0)}(3x^2y - y^3) - \frac{1}{80}G_3^{(2)}(20x^4y - 4y^5) \\
B_{3y} &= G_3^{(0)}(x^3 - 3xy^2) - \frac{1}{80}G_3^{(2)}(4x^5 - 20xy^4) \\
B_{3z} &= G_3^{(1)}(x^3y - xy^3)
\end{aligned} \tag{48}$$

Decapole ($n = 4$):

$$\begin{aligned}
B_{4x} &= G_4^{(0)}(4x^3y - 4xy^3) \\
B_{4y} &= G_4^{(0)}(x^4 - 6x^2y^2 + y^4) \\
B_{4z} &= G_4^{(1)}(x^4y - 2x^2y^3 + y^5/5)
\end{aligned} \tag{49}$$

Dodecapole ($n = 5$):

$$\begin{aligned}
B_{5x} &= G_5^{(0)}(5x^4y - 10x^2y^3 + y^5) \\
B_{5y} &= G_5^{(0)}(x^5 - 10x^3y^2 + 5xy^4) \\
B_{5z} &= 0.
\end{aligned} \tag{50}$$

The complete field components for an arbitrary multipole are then given by

$$\begin{aligned}
B_x &= B_{1x} + B_{2x} + B_{3x} + B_{4x} + B_{5x} \\
B_y &= B_{1y} + B_{2y} + B_{3y} + B_{4y} + B_{5y} \\
B_z &= B_{1z} + B_{2z} + B_{3z} + B_{4z} + B_{5z}
\end{aligned} \tag{51}$$

Particle tracking through the multipole starts by transforming the initial coordinates to system B at the entrance effective edge.

$$\begin{aligned}
 x_B &= -x_A \\
 y_B &= +y_A \\
 z_B &= A - z_A \\
 (v_x)_B &= -(v_x)_A \\
 (v_y)_B &= +(v_y)_A \\
 (v_z)_B &= -(v_z)_A
 \end{aligned}
 \tag{52}$$

The particle is then translated along a straight line to the start of the entrance fringing field at $z = Z11$. The particle differential equations of motion are integrated through the fringing field region to the end of the zone at $z = Z12$.

Particle coordinates are then transformed to system C located at the exit effective edge.

$$\begin{aligned}
 x_C &= -x_B \\
 y_C &= +y_B \\
 z_C &= -(z_B + L) \\
 (v_x)_C &= -(v_x)_B \\
 (v_y)_C &= +(v_y)_B \\
 (v_z)_C &= -(v_z)_B
 \end{aligned}
 \tag{53}$$

The particle differential equations of motion are integrated through the "uniform" field to the start of the exit fringing field zone at $z = Z21$. Following this the particle is tracked through the fringing field region to the end of the zone at $z = Z22$. If the multipole is very short, such that the fringing-field zones overlap, the program integrates backward through the "uniform field" just as for the dipole.

Particle coordinates are then transformed to output system D.

$$z_D = z_C - B. \tag{54}$$

All other coordinates and the velocity components remain unchanged. Finally, the particle is translated along a straight line to the intersection with the plane $z_D = 0$, of system D.

D. MULT. Multipole Corrector

This is an element designed for making dynamic corrections of aberrations in a magnetic spectrometer^{11,12}. It has separate sets of coils for producing dipole, quadrupole, sextupole, octupole, decapole, and dodecapole fields in a rectangular aperture. In the beam direction (z -axis) the field on the median plan is described by a bell shaped curve. In the y -direction it is constant for dipole, proportional to x for quadrupole, etc.:

$$B_y = \frac{B_0[C_0 + C_1(2x/W) + C_2(2x/W)^2 + C_3(2x/W)^3 + C_4(2x/W)^4 + C_5(2x/W)^5]}{1 + C_7[(2z/L)^4 + C_8(L/D)^2(2z/L)^8][1 + C_8(L/D)^2]^{-1}} \quad (55)$$

The field components off the median plane are expressed as Taylor expansions in y with the derivatives calculated numerically, just as for the dipole.

The particle coordinates are initially transformed to coordinate system B which is located at the center of the multipole corrector element (Fig. 16).

$$\begin{aligned} x_B &= x_A \\ y_B &= y_A \\ z_B &= z_A - \left(A + \frac{L}{2}\right) \end{aligned} \quad (56)$$

The corresponding velocity components are unchanged.

The entire multipole corresponds to one integration zone, from $z=Z1$ to $z=Z2$. The particle is first translated through the field-free region to the start of the integration zone at $z=Z1$. Particle motion is then tracked through the non-zero field region terminating at $z=Z2$. The coordinates are then transformed to the output system D at the end of the multipole element.

$$\begin{aligned} x_D &= x_B \\ y_D &= y_B \\ z_D &= z_B - \left(B + \frac{L}{2}\right) \end{aligned} \quad (57)$$

The particle is then translated to the xy -plane of system D.

E. SOLND. Solenoid.

The solenoid subroutine describes the magnetic field in a single-layer (infinitesimally thin) coil. However, no substantial error results from using the routine for any cylindrical coil as long as the thickness of the layer of conductors is reasonably small compared to the diameter. The diameter D specified in the input data should be the mean diameter. The orientation is assumed to be such that the beam direction is along the solenoid axis (Fig. 17).

The field components off-axis as well as on-axis are calculated by integrating Biot-Savart's Law over the surface of the coil. The current density is specified in an indirect way by BF which is the field value in an infinitely long solenoid with the same number of ampere-turns/cm. In other words $BF = 0.4\pi IN/L$.

The magnetic field components for an axially-symmetric ion-free single-layer solenoid are calculated using algebraic expressions as summarized in Ref. 13.

$$B_\rho(i) = \frac{BF}{4\pi} \frac{r_i}{\rho} [2(K - E) - k^2 K] \quad (58)$$

$$B_z(i) = \frac{BF}{4\pi} \frac{4az(i)}{(a + \rho)r_i} [K + \frac{a - \rho}{2a}(\Pi - K)] \quad (59)$$

where $i = L, R$ represents the contribution to each field component due to the left(L) and right(R) hand sources of the finite solenoid.

K, E , and Π are complete elliptic integrals to modulus k , of the first, second, and third kinds, respectively. The length r_i is the maximum distance from a point on the source ring of radius $a = D/2$ to a point on the field ring of radius ρ for each source. In terms of the field point coordinates (x, y, z) and geometrical quantities (Fig. 18);

$$\begin{aligned} \rho^2 &= x^2 + y^2 \\ r_i^2 &= (a + \rho)^2 + z_i^2 \\ k^2 &= 4a\rho/r_i^2 \\ c^2 &= 4a\rho/(a + \rho)^2 ; \text{ parameter of } \Pi \\ z_L &= -(\frac{L}{2} + z) \\ z_R &= +(\frac{L}{2} - z) \end{aligned} \quad (60)$$

The field components for the solenoid are then given by

$$\begin{aligned} B_\rho &= B_\rho(L) - B_\rho(R) \\ B_z &= B_z(L) - B_z(R) \end{aligned} \quad (61)$$

and

$$\begin{aligned} B_x &= B_\rho\left(\frac{x}{\rho}\right) \\ B_y &= B_\rho\left(\frac{y}{\rho}\right) \end{aligned} \quad (62)$$

For field points close to the central axis of the solenoid, $r < 10^{-4}a$, the field components are approximately given by

$$\begin{aligned} B_x &= 0 \\ B_y &= 0 \\ B_z &= BF(\cos \alpha - \cos \beta)/2 \end{aligned} \quad (63)$$

where

$$\begin{aligned}\cos \alpha &= \frac{z_R}{\sqrt{a^2 + z_R^2}} \\ \cos \beta &= \frac{z_L}{\sqrt{a^2 + z_L^2}}\end{aligned}\tag{64}$$

The solenoid has only one integration zone starting a distance Z11 from the beginning of the element and extending to a distance Z22 from the end of the element. Tracking a particle through the solenoid starts by transforming the initial coordinates to system B at the center of the solenoid.

$$\begin{aligned}x_B &= x_A \\ y_B &= y_A \\ z_B &= z_A - A - \frac{L}{2}.\end{aligned}\tag{65}$$

The velocity components are unchanged.

The particle is then translated along a straight line to the start of the entrance fringing field zone at $z=Z11$. The particle differential equations of motion are integrated through the solenoidal field to the end of the exit fringing field zone at $z=Z22$. The coordinates are then transformed to the output system D at the end of the solenoid.

$$\begin{aligned}x_D &= x_B \\ y_D &= y_B \\ z_D &= z_B - B - \frac{L}{2}.\end{aligned}\tag{66}$$

The velocity components remain unchanged. Finally the particle is translated along a straight line to the intersection with the plane $z_D = 0$, of system D.

A solenoid will, of course, not only focus but also twist the beam. If it is desired to see an output with no first order coupling between x and y coordinates, a Shift-Rotate element can be inserted before the end of the complete system.

F. VELs. Velocity Selector.

This subroutine is designed to handle elements with an electric field and a perpendicular magnetic field (Wien filter). As for the electrostatic deflector with cylindrical plates, described earlier, relativistic particle dynamics is used, and the input data (record number 3) must include the rest mass and the charge of the particle. The layout of the coordinate systems is the same as for POLES (Fig. 15).

In the uniform-field region the magnetic field is everywhere in the y -direction and the electric field is in the x -direction. The normal operation of the device assumes that the forces cancel for some mean value of the velocity of the particle, given by $v = E/B$. There is, however, no reason not to use this subroutine for a straight electrostatic deflector (with $B=0$) or a straight magnet (e.g. scanning magnet) with $E=0$.

In the normal design of a velocity selector the electrostatic deflector plates are mounted inside the gap of a homogenous-field magnet with plane-parallel pole surfaces. This device has positive focusing in the x -direction and no focussing in the y -direction. It is possible to design the device such that the focussing is split between the two planes. This is accomplished by making the magnetic gap wedge-shaped. The appropriate field description is produced by use of an n -value and equivalent magnetic radius R_m . The formula for the magnetic field on the midplane is

$$B_y = B_0(1 - nx/R_m) \quad (67)$$

The corresponding formulas for the magnetic field off the midplane are

$$\begin{aligned} (B_y)_{(y \neq 0)} &= B_0 \left[1 - n \left(\frac{x}{R_m} \right) + \frac{n}{2} \left(\frac{R_m}{x + R_m} \right) \left(\frac{y}{R_m} \right)^2 - \frac{n}{24} \left(\frac{R_m}{x + R_m} \right)^3 \left(\frac{y}{R_m} \right)^4 \right] \\ (B_x)_{(y \neq 0)} &= B_0 \left[-n \left(\frac{y}{R_m} \right) - \frac{n}{6} \left(\frac{R_m}{x + R_m} \right)^2 \left(\frac{y}{R_m} \right)^3 \right] \end{aligned} \quad (68)$$

The electric field both on and off the midplane is a constant

$$E_x = E_0. \quad (69)$$

The fringing-field descriptions for both fields are similar to the B -field in the dipole. It is assumed that the entrance and exit angles for the poles are zero. However, there are second and fourth order corrections written into the fringing field description attempting to model the curvature of the iso- B and iso- E lines caused by the limited pole widths. The expression for $E_x(x=0)$ is

$$E_x = E_0 / (1 + e^S) \quad (70)$$

with

$$S = C00 + C01s + C02s^2 + C03s^3 + C04s^4 + C05s^5 \quad (71)$$

and

$$s = z/D + EC2(z/D + 1)y^2/W^2 + EC4y^4/W^4 \quad (72)$$

where W is the width of the electric deflector plates. Similar expressions apply for $B_y(y=0)$:

$$B_y = B_0 / (1 + e^S) \quad (73)$$

with

$$S = C00 + C01s + C02s^2 + C03s^3 + C04s^4 + C05s^5 \quad (74)$$

and

$$s = z/D + BC2(z/D + 1)x^2/W^2 + BC4x^4/W^4 \quad (75)$$

where W is the width of the magnetic pole pieces.

Off the respective planes $x = 0$ and $y = 0$ the fields are calculated by use of Taylor expansions with the necessary derivatives determined numerically, as in the Dipole routine. Since the electrostatic gap normally is smaller than the magnetic gap, the integration steps and the grid size must be tailored to the electrostatic gap, i.e. LF1, etc. $\sim 0.3DE$. An exception to this rule applies if the airgap is tapered as described below.

A serious problem arises in practice for a velocity selector with relatively strong fields if the fringe field from the electrostatic deflector doesn't match that of the magnet¹⁴ such that the condition $v = E/B$ is also fulfilled in the fringe field. The net result is a parallel displacement of the beam at entrance and exit. One remedy is to increase the gap of the electrostatic deflector approximately exponentially at the two ends. The integration step sizes can then be tailored to the magnetic field, i.e. LF1 etc. $\sim 0.3DM$.

The velocity selector consists of three integration zones. Particle tracking starts by transforming the initial coordinates to system B at the entrance effective edge.

$$\begin{aligned} x_B &= -x_A \\ y_B &= +y_A \\ z_B &= A - z_A \\ (v_x)_B &= -(v_x)_A \\ (v_y)_B &= +(v_y)_A \\ (v_z)_B &= -(v_z)_A \end{aligned} \quad (76)$$

The particle is then translated along a straight line to the start of the entrance fringing field zone at $z = Z11$. The particle differential equations of motion are integrated through the fringing field region to the end of the zone at $z = Z12$.

Particle coordinates are then transformed to system C located at the exit effective edge.

$$\begin{aligned} x_C &= -x_B \\ y_C &= +y_B \\ z_C &= -(z_B + L) \\ (v_x)_C &= -(v_x)_B \\ (v_y)_C &= +(v_y)_B \\ (v_z)_C &= -(v_z)_B \end{aligned} \quad (77)$$

The particle differential equations of motion are integrated through the "uniform" field to the start of the exit fringing field zone at $z = Z21$. Following this the particle is tracked through the fringing field region to the end of the zone at $z = Z22$. If the velocity-selector is very short, such that the fringing-field zones overlap, the program integrates backwards through the "uniform field" just as for the dipole.

Particle coordinates are then transformed to output system D.

$$z_D = z_C - B \quad (78)$$

All other coordinates and the velocity components remain unchanged. Finally the particle is translated along a straight line to the intersection with the plane $z_D = 0$, of system D.

G. LENS. Transformation Matrix.

This subroutine performs a multiplication of the beam matrix (i.e. each individual ray separately) with a transfer matrix specified by the input data. The first order part is

$$\begin{array}{cccc} x/x & x/\theta & 0 & 0 \\ \theta/x & \theta/\theta & 0 & 0 \\ 0 & 0 & y/y & y/\phi \\ 0 & 0 & \phi/y & \phi/\phi \end{array} \quad (79)$$

If the lens is thin and rotationally symmetric, then one has $x/x = y/y$, etc. Chromatic and spherical aberrations can then also be handled rather simply as follows:

a) Spherical Aberration

$$\Delta\theta = CS(\theta/x)^4(x^2 + y^2)x \quad (80)$$

$$\Delta\phi = CS(\phi/y)^4(x^2 + y^2)y$$

with CS being the spherical aberration coefficient measured in cm. These formulas make CS a coefficient as close as possible to the spherical aberration used in electron optics. CS is normally negative for a positive lens.

b) Chromatic Aberration

The lens focal length is corrected for the particle energy according to

$$\begin{aligned} (\theta/x) &= (\theta/x)_0 (E_0/E)^n \\ (\phi/y) &= (\phi/y)_0 (E_0/E)^n \end{aligned} \quad (81)$$

E_0 is an input reference energy. For an Einzel (thin) lens $n = 1$. If the particle mass is unspecified so that E = momentum, then $n \approx 2$ for non-relativistic energies. For $n = 0$ or $E_0 = E$ (default), (θ/x) and (ϕ/y) will be constant.

Note: Neither the time variable t nor the total system length are updated by the LENS element even if non-zero coefficients x/θ and y/ϕ are used to represent a finite lens thickness. In such cases, there can also be large artificial discontinuities in both x and y at the location of the lens.

H. SHRT. Shift-Rotate.

This subroutine executes a transformation to a new coordinate system. The position and/or orientation of the entire part of the optical system that follows SHRT is changed by specified amounts relative to the preceding part. The order of the transformation is the same as the order of the entries. This means that translations are performed before rotations and that the rotation ψ_x (about the x -axis) is performed before ψ_y , etc.

If two or more shifts or twists are called for, in a different order than specified above, it is necessary to use more than one SHRT element to achieve the desired coordinate transformation.

If Δx , Δy , and Δz represent the desired translations along the respective axes, the resulting transformations are given by

$$\begin{aligned}x_2 &= x_1 - \Delta x \\y_2 &= y_1 - \Delta y \\z_2 &= z_1 - \Delta z\end{aligned}\tag{82}$$

In the case of a coordinate rotation ψ_x about the x -axis, the transformation is given by

$$\begin{aligned}y_2 &= +y_1 \cos \psi_x + z_1 \sin \psi_x \\z_2 &= -y_1 \sin \psi_x + z_1 \cos \psi_x \\(v_y)_2 &= +(v_y)_1 \cos \psi_x + (v_z)_1 \sin \psi_x \\(v_z)_2 &= -(v_y)_1 \sin \psi_x + (v_z)_1 \cos \psi_x\end{aligned}\tag{83}$$

For a coordinate rotation ψ_y about the y -axis, the transformation is given by

$$\begin{aligned}x_2 &= x_1 \cos \psi_y - z_1 \sin \psi_y \\z_2 &= x_1 \sin \psi_y + z_1 \cos \psi_y \\(v_x)_2 &= (v_x)_1 \cos \psi_y - (v_z)_1 \sin \psi_y \\(v_z)_2 &= (v_x)_1 \sin \psi_y + (v_z)_1 \cos \psi_y\end{aligned}\tag{84}$$

Finally, for a coordinate rotation ψ_z about the z -axis, the transformation is given by

$$\begin{aligned}x_2 &= +x_1 \cos \psi_z + y_1 \sin \psi_z \\y_2 &= -x_1 \sin \psi_z + y_1 \cos \psi_z \\(v_x)_2 &= +(v_x)_1 \cos \psi_z + (v_y)_1 \sin \psi_z \\(v_y)_2 &= -(v_x)_1 \sin \psi_z + (v_y)_1 \cos \psi_z\end{aligned}\tag{85}$$

I. DRIFT. Field-Free Drift.

Normally drifts between active elements in RAYTRACE are handled by the parameters A and B, usually referred to as "object" and "image" distances for the element. Actually, these distances simply define convenient positions between elements to print out the coordinates of a ray. Sometimes there is a need for a separate element to represent a drift space. DRIFT fills this need. It performs a simple transformation:

$$\begin{aligned}t_2 &= t_1 + (DZ - z_1)/v_z \\ \Delta t &= t_2 - t_1 \\ x_2 &= x_1 + v_x \Delta t \\ y_2 &= y_1 + v_y \Delta t \\ z_2 &= 0\end{aligned}\tag{86}$$

with \vec{v} unchanged.

J. COLL. Collimator.

This subroutine is designed to eliminate rays that would not pass through the real-life system. None of the subroutines described earlier has any provision for stopping a ray that would not make it through the system in practice, for instance by exceeding $y = D/2$ in a dipole.

The collimator can be either rectangular or elliptic. The other input data are:

- a) Position of the center of the collimator
- b) Half-axes of the rectangle or ellipse.

A ray which has an amplitude outside that permitted by the aperture will be stopped at that point. A statement printed in the output reads: "Stopped. Exceeds rectangular (elliptical) collimator dimensions."

References

1. K.L. Brown, D.C. Carey, Ch. Iselin, and F. Rothacker, TRANSPORT, A Computer Program for Designing Charged Particle Beam Transport Systems, SLAC-91, NAL-91, and CERN 80-04
2. MOTER, an optimization program developed at Los Alamos, A. Thiessen, private communication.
3. H. Ikegami, S. Morinobu, I. Katayama, M. Fujiwara, Y. Fujita, and H. Ogata, RCNP Annual Report 1976 (Osaka University).
4. W. B. Hermannsfeldt, Nucl. Instr. and Meth. 187, 245 (1981).
5. C. M. Braams, Nucl. Instr. and Meth. 26, 83 (1964).
6. POISSON: J.S. Colonias and J.H. Dorst, UCRL-16382 (1965). A.M. Winslow, Journal of Computer Physics 1, 149 (1967). E. Furfine et. al., SLAC-56 (1966).
7. H. A. Enge, Focusing of Charged Particles, Vol. 2, p. 203, A. Septier, editor, Academic Press Inc., New York, 1967.
8. H. A. Enge, Rev. of Sci. Instr. 35, 278 (1964).
9. H. A. Enge, Rev. of Sci. Instr. 34, 385 (1964).
10. A multipole designed by H. A. Enge and S. B. Kowalski for use in a QDQ spectrometer at Indiana University.
11. H. J. Scheerer, H. Vonach, M. Löffler, A. v.d. Decken, M. Goldschmidt, C. A. Wiedner, and H. A. Enge, Nucl. Instr. and Meth., 136, 213 (1976).
12. H. Ikegami, Nucl. Instr. and Meth., 187, 13 (1981).
13. M. W. Garrett, Journal of Appl. Phys. 34, 2567 (1963).
14. M. Salomaa and H. A. Enge, Nucl. Instr. and Meth., 145, 279 (1977).

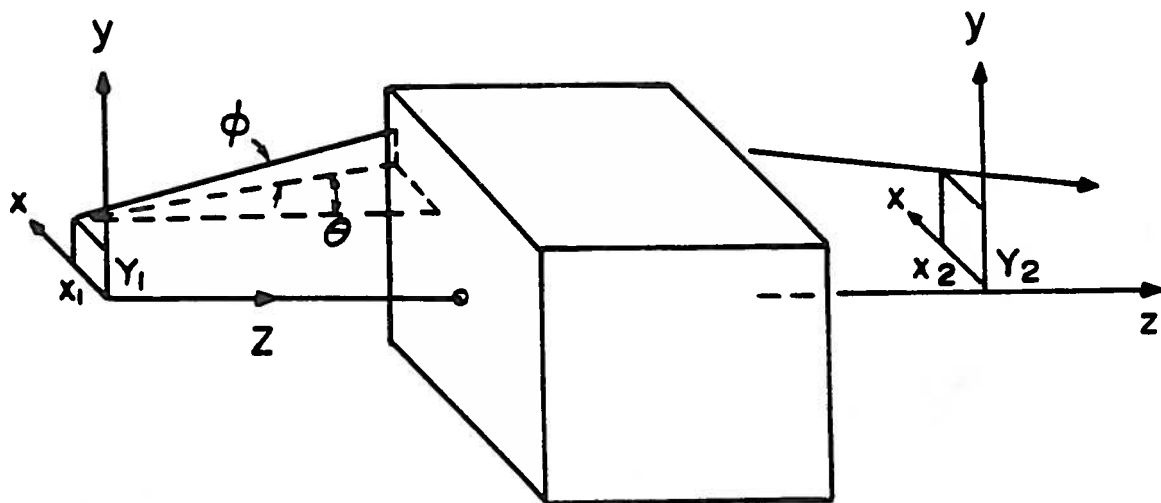


Figure 1. Input and output coordinates for an arbitrary ion-optical system consisting of any number of individual elements.

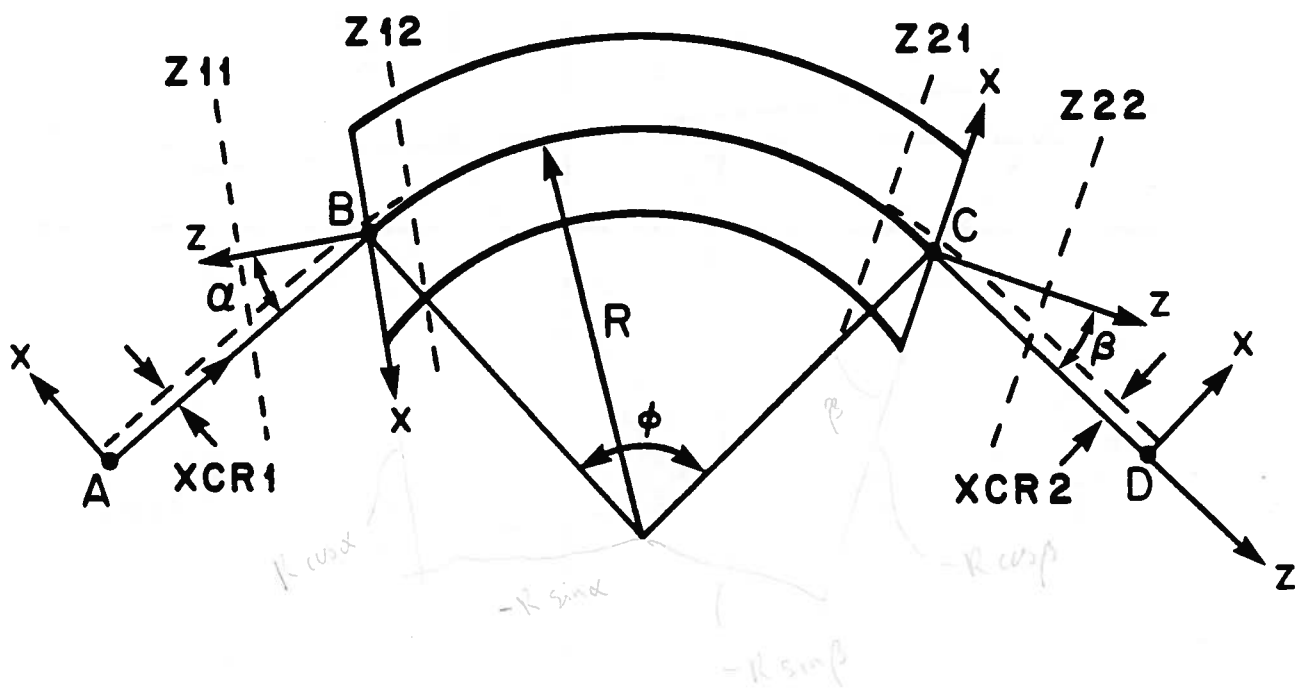


Figure 2. Definition of the most important parameters used in the DIPOLE subroutine.

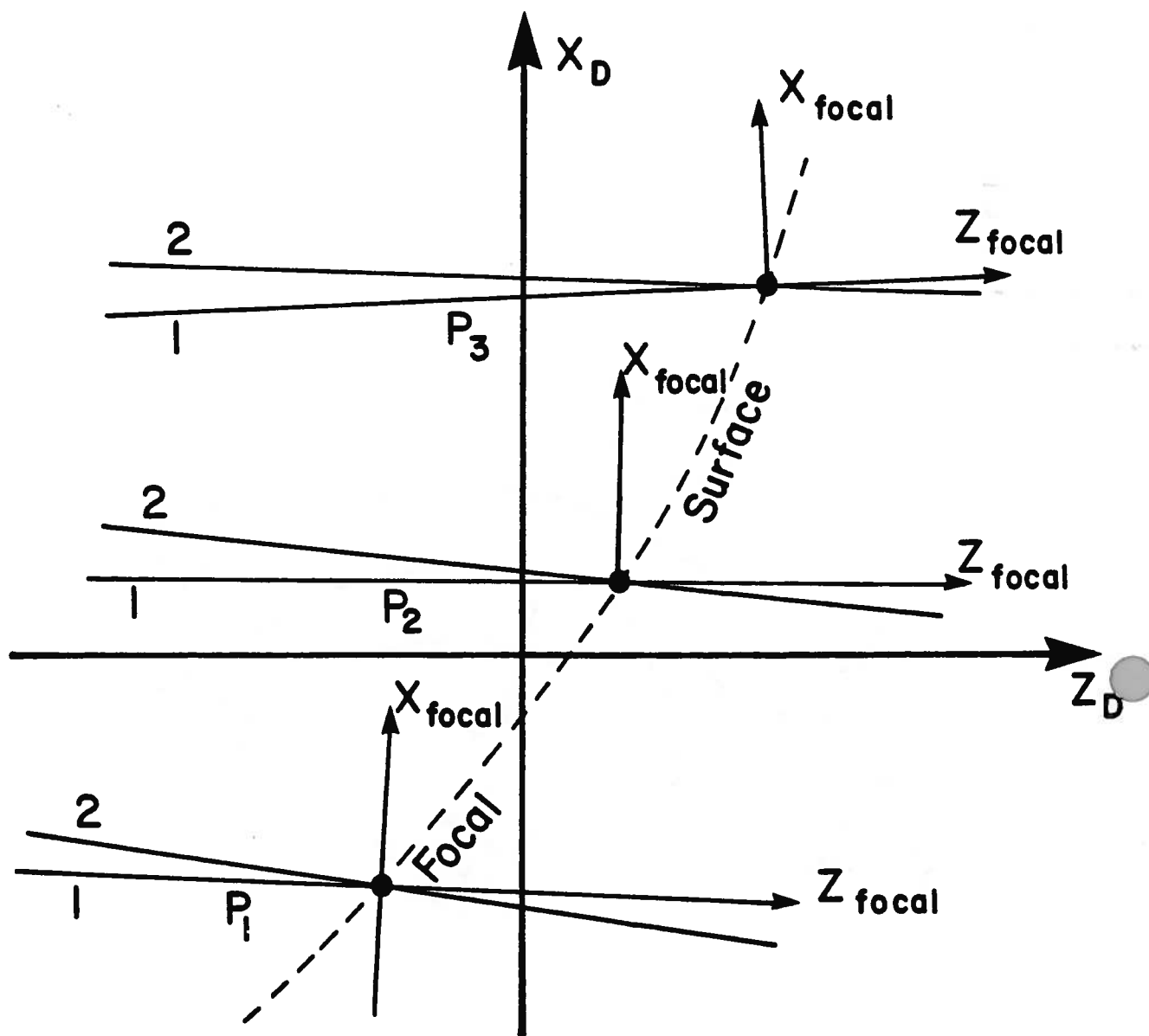


Figure 3. Output coordinate system formed at the intersection of Ray 1 and Ray 2 for three different momenta.

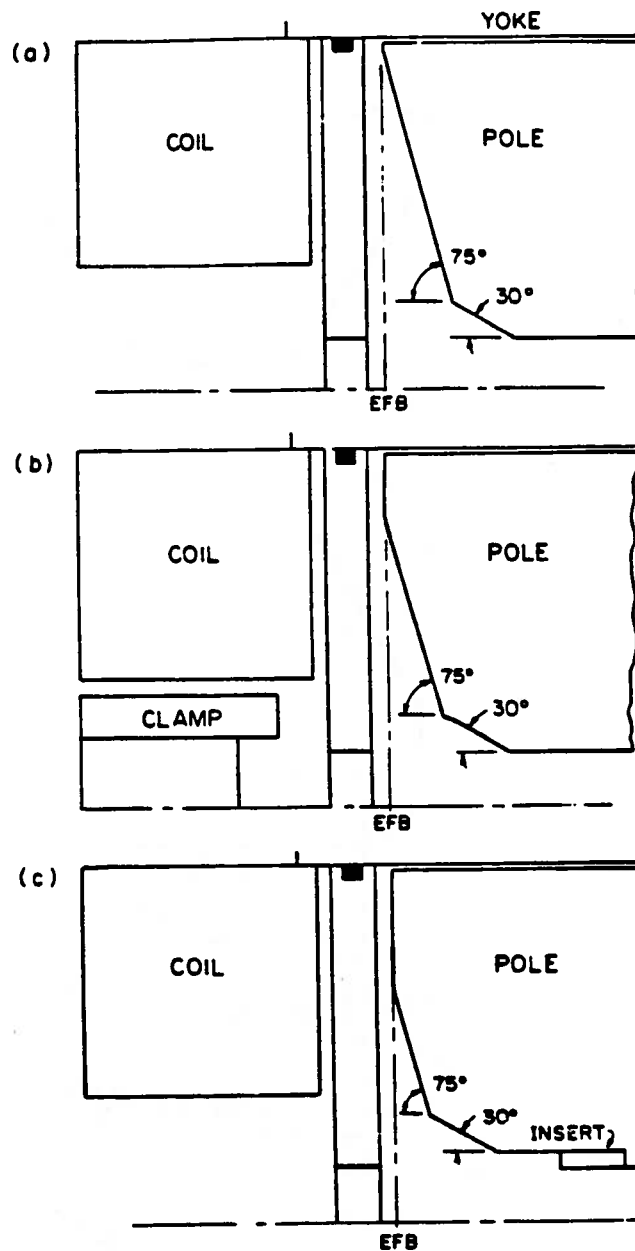


Figure 4. Rogowski pole profiles for three different cases. All are designed such that the Effective-Field Boundary (EFB) approximately coincides with the upper portion of the pole.

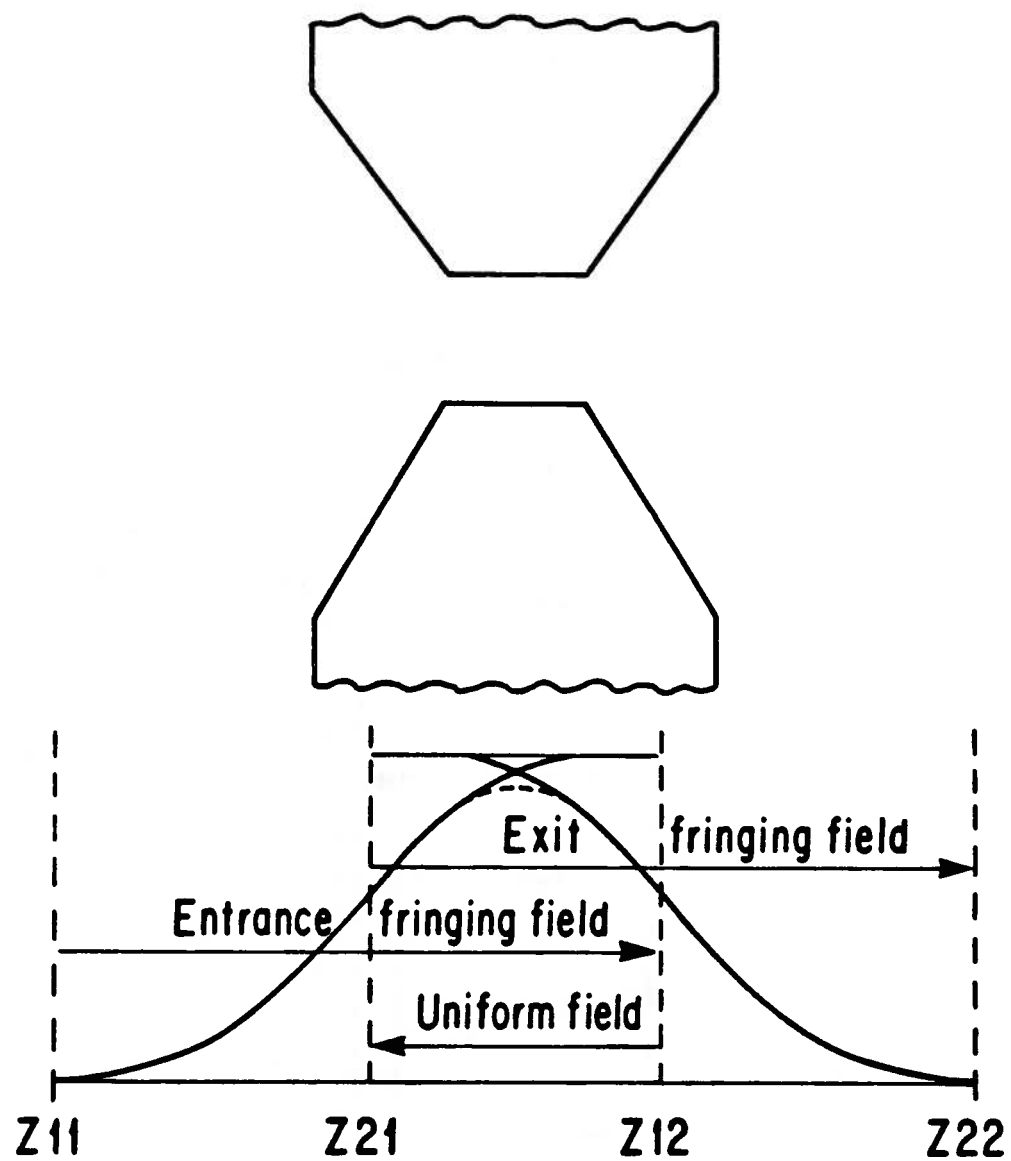


Figure 5. Overlapping fringing-field zones. The dashed curve indicates approximately what the net effect will be on the particle by the "backward" integration.

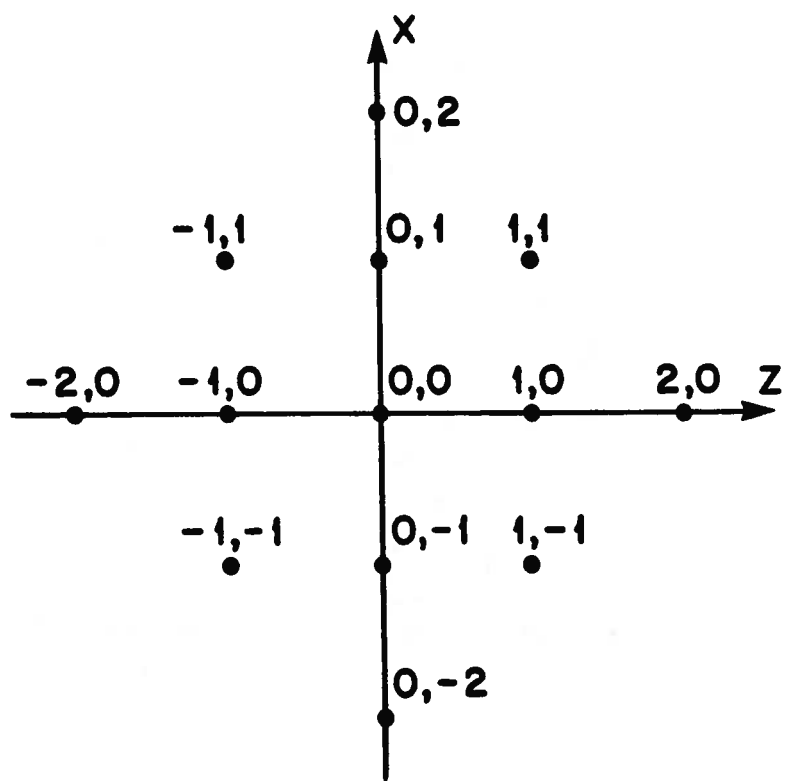


Figure 6. Thirteen-point grid used to determine numerical derivatives of B_y in the median plane.

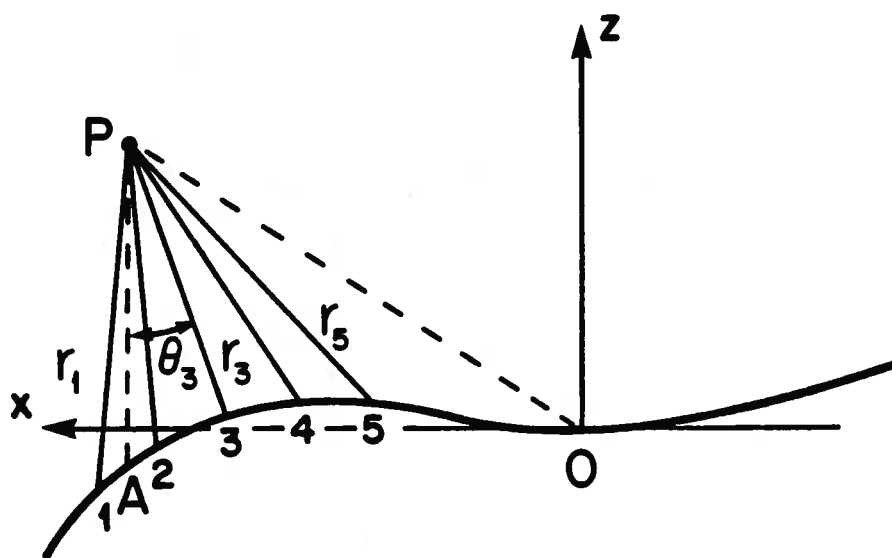


Figure 7. A spray of five “feeler rays” used to determine a representative distance to the EFB and thereby the value of B_y .

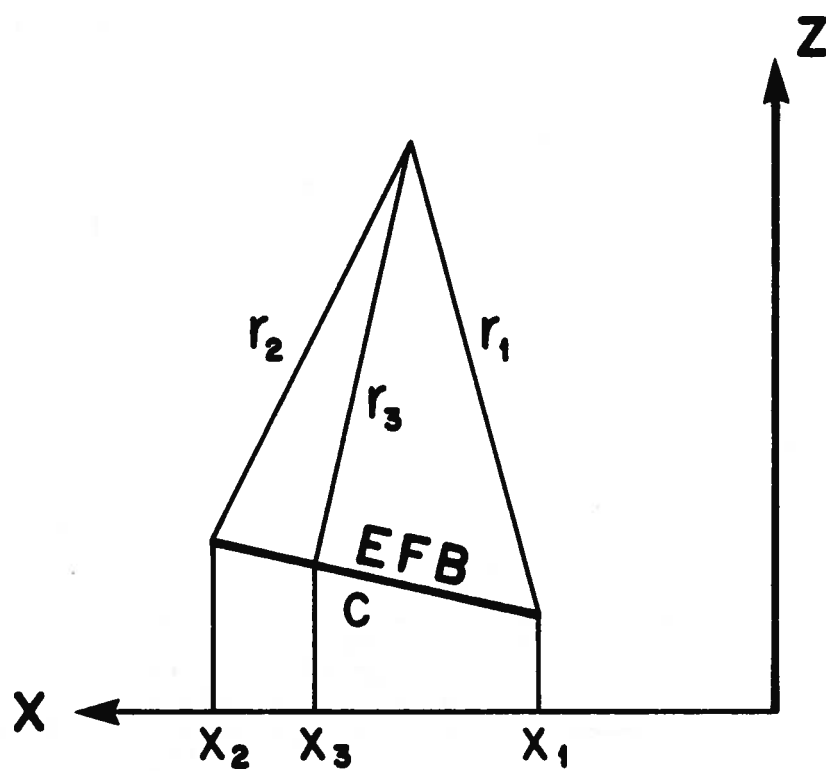


Figure 8. Trigonometry used to evaluate the shortest distance between the field point and the boundary.

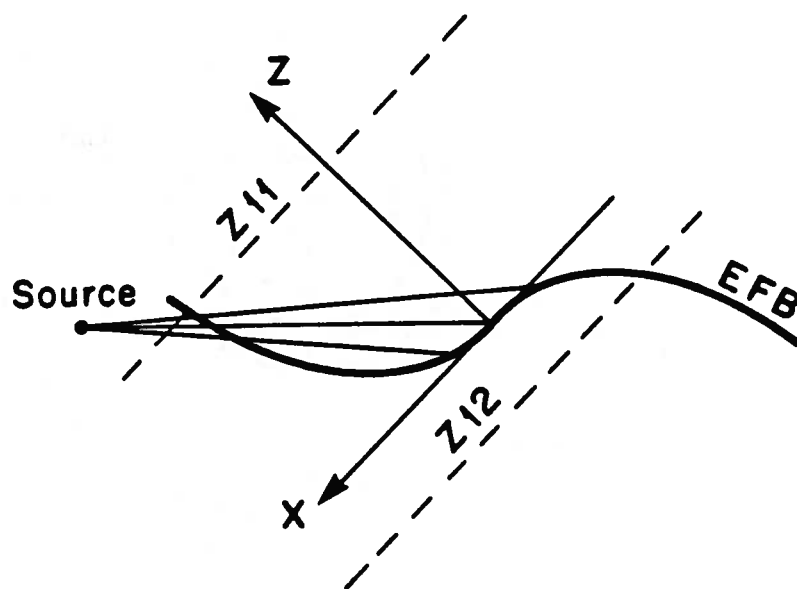


Figure 10. Possible result of an indiscriminate use of the parameters SO_2 , etc. that describe the shape of the EFB.

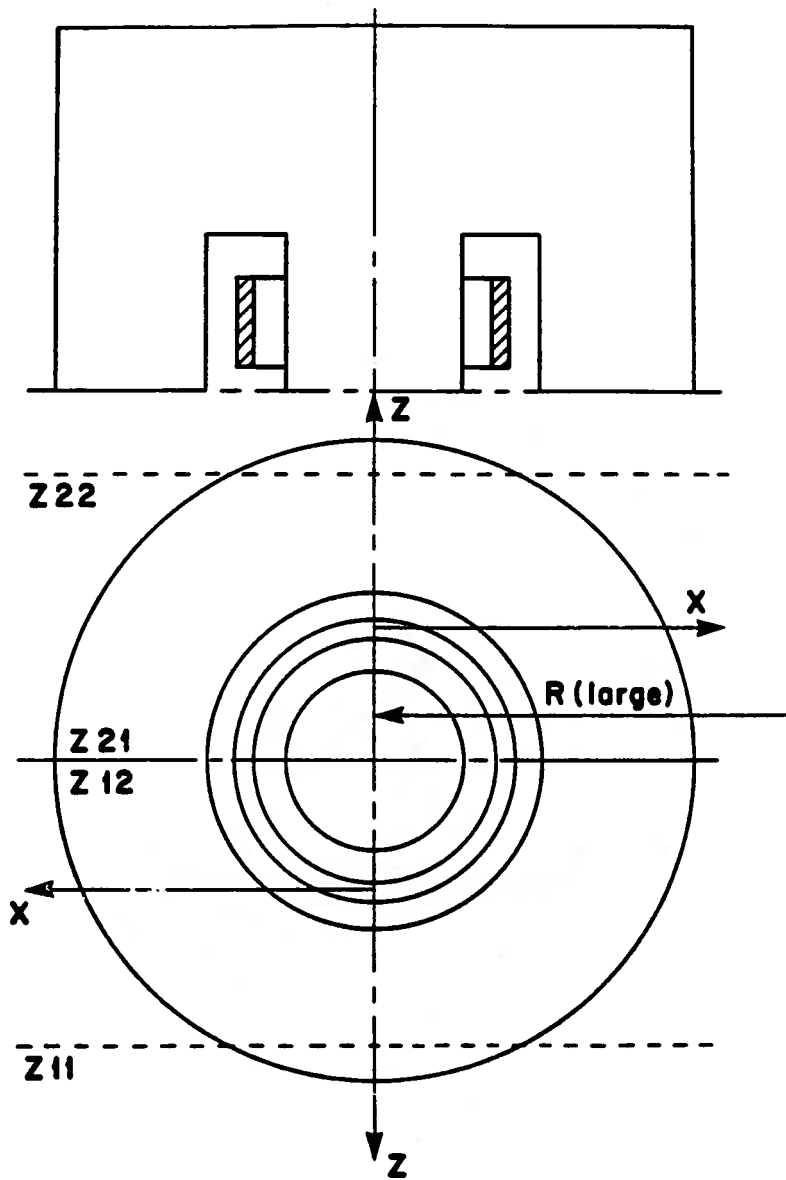


Figure 11. Magnetic dipole with circular poles (MTYP = 5).

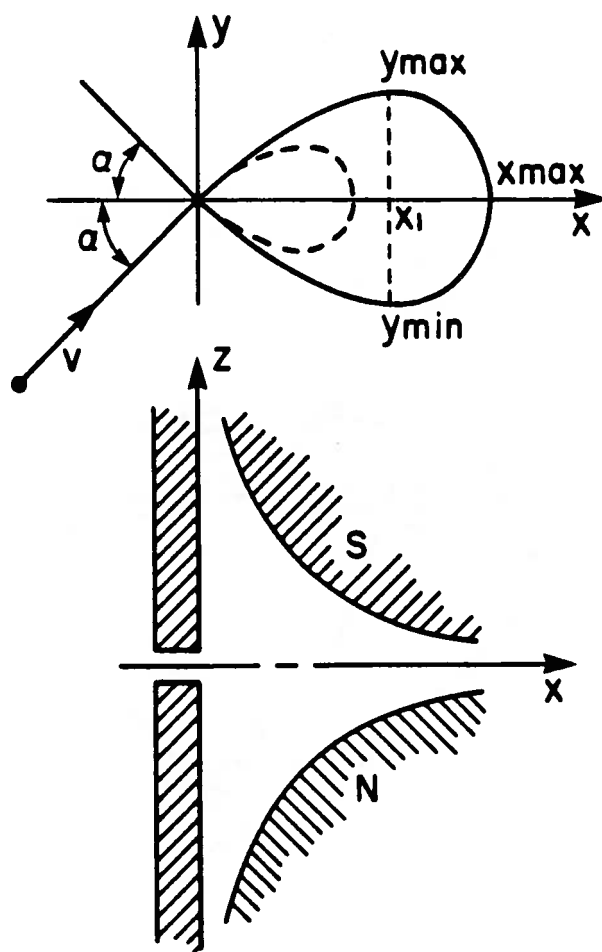


Figure 12. Pretzel magnet (MTYP = 6).

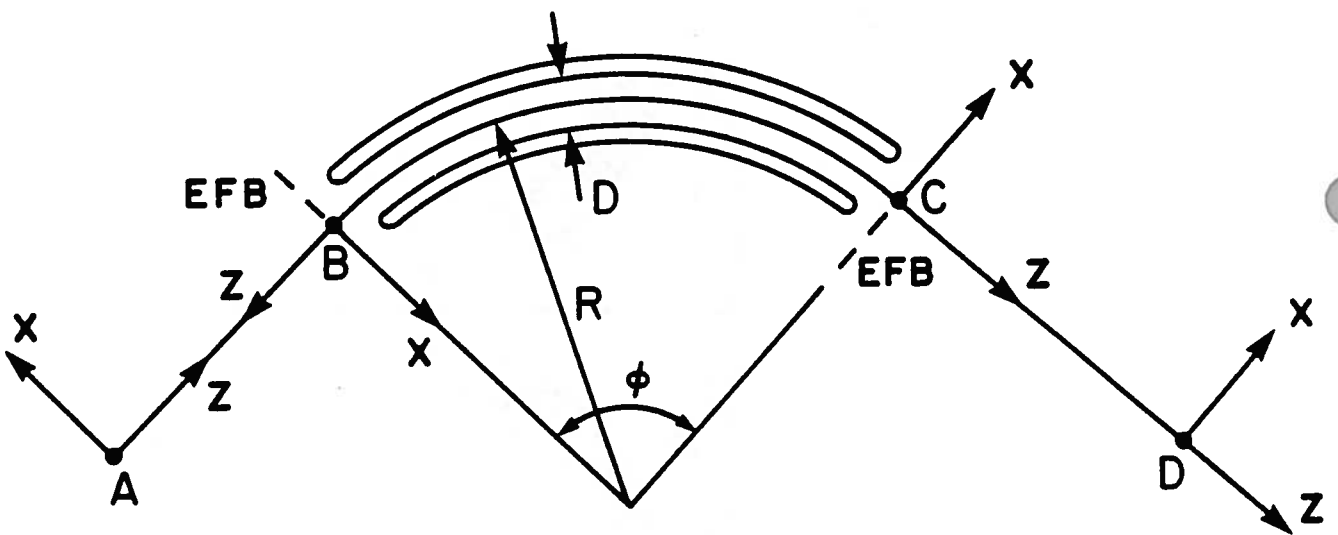


Figure 13. Electrostatic cylinder deflector and the geometry of the coordinate systems used in EDIPL.

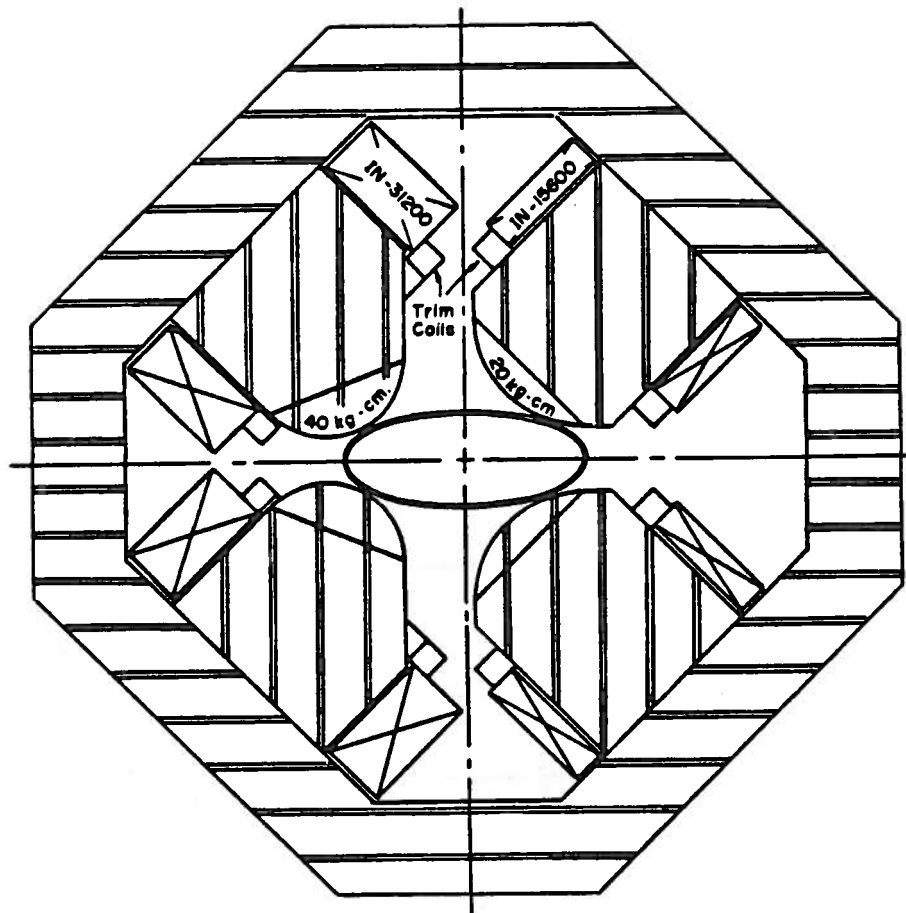


Figure 14. An example of a multipole where the higher-order terms produce strong perturbations on the normal quadrupole contours. In this case the ampere-turns are also different between the left and right pole pairs. The fields at the nominal aperture radius $R = 10$ cm are $BQ = 8.40$ kG, $BH = -3.40$ kG, $BO = 1.56$ kG, and $BD = 0.60$ kG.

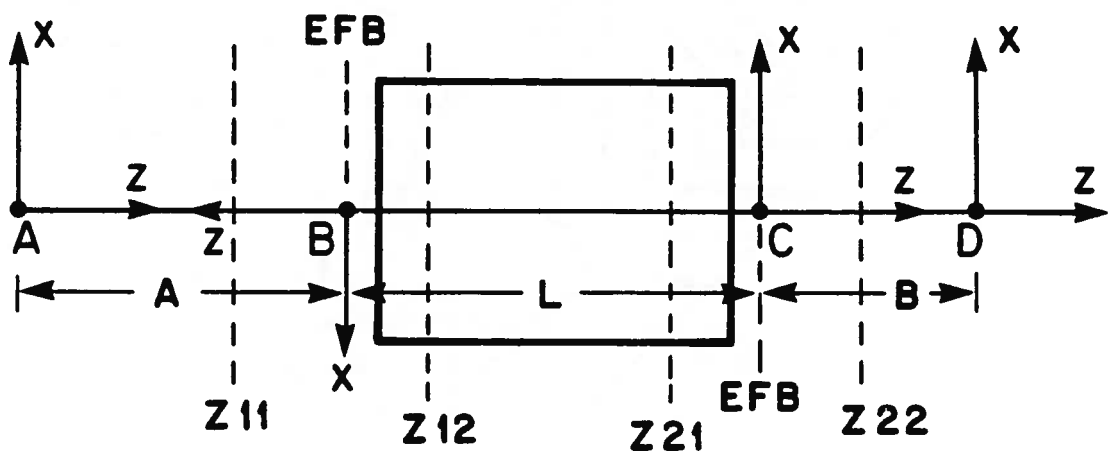


Figure 15. Coordinate systems used in subroutine POLES.

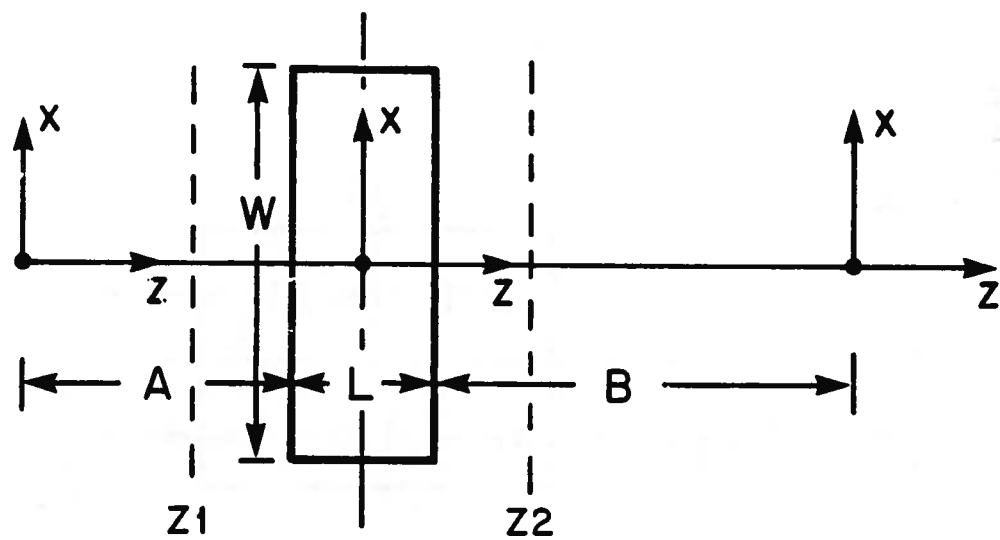


Figure 16. Coordinate systems used in subroutine MULT (Multipole Corrector).

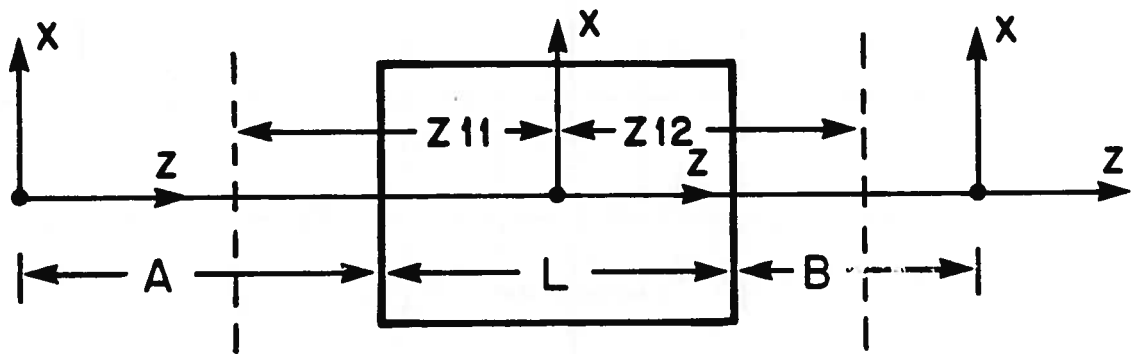


Figure 17. Coordinate systems used in subroutine SOLENOID. Note: in this case L is the physical length of the solenoid, i.e. the concept of an effective-field boundary is not used.

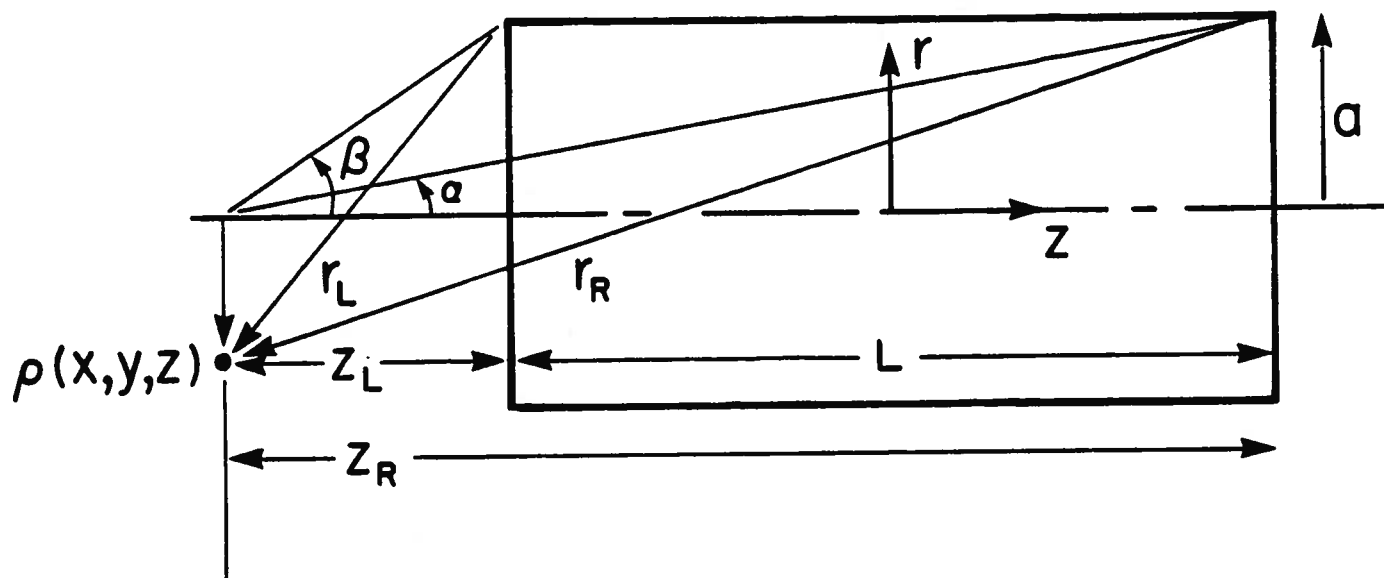


Figure 18. Geometry used in calculating the field of the solenoid.



Appendix 1. Input Parameters Description

I. Element

Type	Code	Records
Sentinel	SENT	1
Dipole	DIPO	12
ES Deflector	EDIP	8
Multipole	POLE	8
Multipole Corrector	MULT	6
Solenoid	SOLE	4
Velocity Selector	VELS	11
Lens	LENS	2
Shift-Rotate	SHRT	2
Drift	DRIF	2
Collimator	COLL	2

A. Problem Definition (3 records)

Record	Variable	Format
1	NTITLE - Problem or other identifying description	20A4
2	NR - Number of rays to be traced per energy. NP - Number of integration steps per printed line NP=100+N - Print out every Nth step for central energy only. NP>200 - Omit all intermediate printout. NSKIP - Transfer matrix option (see Table below) JFOCAL - Output coordinate axes option. JFOCAL=0 - Intersection of Rays 1 and 2, or their projections on the zz plane, is used to determine the origin and orientation of the output coordinate system. z -axis oriented along direction of Ray 1. JFOCAL=1 - Origin of output coordinate system fixed at $z_D = 0$, where D denotes the final fixed coordinate system in the last element. The z -axis is oriented along the direction of Ray 1. The subroutines used for calculating the orbits through optical elements in RAYTRACE in general use either three or four fixed coordinate systems per element. The first and last are referred to as systems A and D. JFOCAL=2 - Output coordinate system is the D-axis system of the final element. JMTRX - Not used. JNR - A flag which is used to determine whether the rays to be traced appear as input in the data stream or are generated automatically by the program JNR=0 - Individual input rays appear in the data stream immediately following the SENTINEL terminator. JNR=2 - Input record after SENTINEL defines a pair of paraxial rays. JNR=6 - Input record after SENTINEL defines 6 rays describing the usual midplane point source problem. JNR=14 - Input record after SENTINEL defines 14 rays describing the full solid angle point source problem.	7I5

read (5,102) NR, IP, NSKIP, JFOCAL, JPRT, JNR, MPLT

A. Problem Definition (3 Records) - Continued

Record	Variable	Format															
	JNR=46 - Input record after SENTINEL defines 46 rays describing the full solid angle general non-point source problem.																
	NPLT - Plotting option. NPLT=0 - Normal. NPLT≠0 - Generate plot file.																
	Transfer Matrix Options																
	<table> <tr> <th>Matrix</th><th>NR</th><th>NSKIP</th></tr> <tr> <td>Point Source (Midplane)</td><td>$6 \leq NR < 14$</td><td>0</td></tr> <tr> <td>Point Source (Full Solid Angle)</td><td>$14 \leq NR < 46$</td><td>0</td></tr> <tr> <td>Standard</td><td>≥ 46</td><td>0</td></tr> <tr> <td>None</td><td>Any</td><td>≠ 0</td></tr> </table>	Matrix	NR	NSKIP	Point Source (Midplane)	$6 \leq NR < 14$	0	Point Source (Full Solid Angle)	$14 \leq NR < 46$	0	Standard	≥ 46	0	None	Any	≠ 0	
Matrix	NR	NSKIP															
Point Source (Midplane)	$6 \leq NR < 14$	0															
Point Source (Full Solid Angle)	$14 \leq NR < 46$	0															
Standard	≥ 46	0															
None	Any	≠ 0															
3	Energy - Particle kinetic energy in MeV for first calculation DEN - Change in particle energy for successive runs XNEN - Number of complete runs with successive energy changes including first run. Default = 1. PMASS - Mass of particle (AMU) Q - Charge state of particle, units of electron charge. - If mass and charge are not specified, i.e. PMASS=0 and Q=0, the program assumes a relativistic particle with Q=1, v=c, and p=E in MeV/c.	5F10.5															

B. Dipole (12 records)

Record	Variable	Format
1	DIPOLE	A4
2	<p>LF1 - Entrance fringing field integration step size (cm)</p> <p>LU1 - Uniform field integration step size (cm)</p> <p>LF2 - Exit fringing field integration step size (cm)</p> <p>DG - Differential step size used in determining off mid-plane components of B using numerical differential methods. Recommended for all four step sizes: 0.3D (D=Gap) although LU1 can be made larger to save computer time. For MTYP=6, DG serves another function. See Sec. V. A.</p> <p>MTYP - Magnetic dipole option</p> <p>MTYP=0,1 - Uniform field dipole. Fringing field determined by calculation of the distance to the effective field boundary in the z-direction.</p> <p>MTYP=2 - Uniform field dipole. Fringing field determined as described in Sec. V.A.</p> <p>MTYP=3 - Non-uniform field dipole with n-value and second-, third-, and fourth-order corrections. Fringing field determined as for MTYP=2, but including n-value, etc.</p> <p>MTYP=4 - Non-uniform field dipole - cylindrical geometry. Similar to MTYP=3 but better suited for purely conical pole pieces. This option is used to describe magnets with wedge-shaped gaps ("CLAMSHELL") by making R large, PHI small, and by setting BET1=GAMA=DELT=0 but n≠0, and normally large because R is artificially large.</p> <p>MTYP=5 - Uniform field dipole, circular pole option.</p> <p>MTYP=6 - Pretzel magnet option.</p> <p>IMAP - Array number for generating and identifying fringing field array maps. If IMAP=0, maps are not generated and the field components are calculated directly for each point, i.e. four times for each integration step. Two dipoles with identical values of IMAP will share a common array. IMAP≤5.</p>	6F10.5
3	<p>A - Distance (cm) from origin of system A (initial) to system B (situated at entrance edge EFB of magnetic element)</p>	5F10.5

B. Dipole (12 records) - Continued

Record	Variable	Format
	B - Distance (cm) from origin of system C (situated at exit edge EFB of magnetic element) to origin of output system D	
	D - Gap width (cm)	
	R - Radius of curvature (cm) used in geometrical construction of layout	
	BF - Nominal value of the field on the central radius R (Tesla)	
4	PHI - Angular extent between the EFB of system B and that of system C (degrees). Nominally equivalent to the bend angle	3F10.5
	ALPHA - Angle between the central trajectory and the normal to the effective field boundary (EFB) at entrance (degrees)	
	BETA - Angle between the central trajectory and the normal to the exit boundary (degrees). Both ALPHA and BETA are positive when the normals are outside the orbit for positive transverse plane focussing.	
5	NDX - 'n-value', of field index for non-uniform field magnets (first-order term).	4F10.5
	BET1 - ' β -value', of field index for non-uniform field magnets (second-order term).	
	GAMA - ' γ -value', of field index for non-uniform field magnets (third-order term).	
	DELT - ' δ -value', of field index for non-uniform field magnets (fourth-order term).	
6	Z11 - Integration limit (cm) defining the start of the entrance fringing field zone in coordinate system B. Normally positive.	4F10.5
	Z12 - Integration limit (cm) defining the termination of the entrance fringing field zone in coordinate system B. Normally negative.	
	Z21 - Integration limit (cm) defining the start of the exit fringing field zone in coordinate system C. Normally negative.	
	Z22 - Integration limit (cm) defining the termination of the exit fringing field zone in coordinate system C. Normally positive.	

B. Dipole (12 records) - Continued

Record	Variable	Format
7	C00	6F10.5
	C01	
	C02	
	C03	
	C04	
	C05	
8	C10	6F10.5
	C11	
	C12	
	C13	
	C14	
	C15	
9	BR1	6F10.5
	BR2	
	XCR1	
	XCR2	
	DELS1	
	DELS2	

B. Dipole (12 records) - Continued

Record	Variable	Format
10	RAP1 - Inverse radius of curvature of entrance boundary (cm^{-1}). Convex surfaces are positive.	2F10.5
	RAP2 - Inverse radius of curvature of exit boundary (cm^{-1}). Convex surfaces are positive. In the program, except for MTYP=5, circles described by RAP1 and RAP2 are approximated with an eighth-order power series.	
	WDE - Mechanical width of the entrance pole boundary. Used only when IMAP is non-zero.	
	WDX - Mechanical width of the exit pole boundary. Used only when IMAP is non-zero.	
11	S02 - Coefficients used in description of entrance boundary curvature. Contributions of RAP1 are added to those of S02, S04, S06, and S08.	7F10.5
	S03	
	S04	
	S05	
	S06	
	S07	
	S08	
12	S12 - Coefficients used in description of exit boundary curvature. Contributions of RAP2 are added to those of S12, S14, S16, and S18.	7F10.5
	S13	
	S14	
	S15	
	S16	
	S17	
	S18	

C. Electrostatic Deflector (8 records)			
Record	Variable		Format
1	EDIP		A4
2	LF1	- Entrance fringing field integration step size (cm).	5F10.5
	LU1	- Uniform field integration step size (cm).	
	LF2	- Exit fringing field integration step size (cm). Recommended for these three step sizes: 0.3D (D=Gap) although LU1 can be larger to save on computer time.	
	DG	- Differential step size used in determining off mid-plane components of B using numerical differential methods. Recommendation: DG=0.2D or smaller.	
3	A	- Distance (cm) from origin of system A (initial) to system B (situated at entrance edge EFB of electrostatic element).	5F10.5
	B	- Distance (cm) from origin of system C (situated at exit edge EFB of electrostatic element) to origin of output system D.	
	D	- Gap width (cm)	
	R	- Radius of curvature (cm) used in geometrical construction of layout	
	EF	- Electric field on the central orbit (kV/cm)	
4	PHI	- Angular extent between the EFB of system B and that of system C (degrees). Nominally equivalent to the bend angle.	5F10.5
5	EC2	- Coefficients describing second and fourth order curvature of the iso-field lines on the median plane in the fringing field regions — due to finite width of the plates.	5F10.5
	EC4		
	WE	- Plate width (cm).	
	WC	- Not presently used.	
6	Z11	- Integration limit (cm) defining the start of the entrance fringing field zone in coordinate system B. Normally positive.	4F10.5
	Z12	- Integration limit (cm) defining the termination of the entrance fringing field zone in coordinate system B. Normally negative.	
	Z21	- Integration limit (cm) defining the start of the exit fringing field zone in coordinate system C. Normally negative.	

C. Electrostatic Deflector (8 records)			
<u>Record</u>	<u>Variable</u>		<u>Format</u>
	Z22	- Integration limit (cm) defining the termination of the exit fringing field zone in coordinate system C. Normally positive.	
7	C00	- Coefficients used in the expansion of the fringing field fall-off at the entrance of the electrostatic deflector.	6F10.5
	C01		
	C02		
	C03		
	C04		
	C05		
8	C10	- Coefficients used in the expansion of the fringing field fall-off at the exit of the electrostatic deflector.	6F10.5
	C11		
	C12		
	C13		
	C14		
	C15		

D. Multipole (8 records)

Record	Variable	Format
1	POLES	A4
2	LF1 - Entrance fringing field integration step size (cm). LU1 - Uniform field integration step size (cm). LF2 - Exit fringing field integration step size (cm). Recommended for all three step sizes: 0.3R	3F10.5
3	A - Distance (cm) from origin of system A (initial) to system B (situated at EFB of entrance edge of magnetic element). B - Distance (cm) from origin of system C (situated at EFB of exit edge of magnetic element) to origin of output system D. L - Effective length (cm) of magnetic element. R - Aperture radius (cm).	4F10.5
4	BQ - Quadrupole component at $r=R$ (Tesla). BH - Hexapole component at $r=R$ (Tesla). BO - Octapole component at $r=R$ (Tesla). BD - Decapole component at $r=R$ (Tesla). BDD - Dodecapole component at $r=R$ (Tesla).	5F10.5
5	Z11 - Integration limit (cm) defining the start of the entrance fringing field zone in coordinate system B. Normally positive. Z12 - Integration limit (cm) defining the termination of the entrance fringing field zone in coordinate system B. Normally negative. Z21 - Integration limit (cm) defining the start of the exit fringing field zone in coordinate system C. Normally negative. Z22 - Integration limit (cm) defining the termination of the exit fringing field zone in coordinate system C. Normally positive.	4F10.5
6	C00 - Coefficients used in the expansion of the C01 fringing field fall-off at the entrance C02 of the magnetic element. C03 C04 C05	6F10.5

D. Multipole (8 records) - Continued

Record	Variable	Format
7	C10 - Coefficients used in the expansion of the C11 fringing field fall-off at the exit of the C12 magnetic element. C13 C14 C15	6F10.5
8	FRH - Fractional radius of multipoles, in terms of FRO quadrupole radius, used in calculating fringing field FRD fall-off, <i>e.g.</i> FRH=0.9 makes the hexapole fall-off FRDD 0.9^{-1} times faster with distance from the EFB than the quadrupole field. DSH - A correction for the effective length of individual DSO multipole elements relative to the quadrupole. DSD A positive DS represents a displacement inward of DSDD the EFB at the entrance and exit in units of R.	8F10.5

E. Multipole Corrector (6 records)

Record	Variable	Format
1	MULT	A4
2	LF - Integration step size (cm) DG - Differential step size (cm) used in determining off-midplane components of B using a numerical differential technique. Recommended for both step sizes: 0.3D	3F10.5
3	A - Distance (cm) from origin of system A (initial) to coordinate system situated at centre of multipole element. B - Distance (cm) from coordinate system situated at centre of multipole element to origin of output system D. L - Length of the Multipole Corrector (cm). W - Width (cm) of multipole element. D - Gap (cm) of multipole element. BF - Nominal value of field at $x = W/2$ and $z = 0$, i.e. the value the field at $x = W/2$ will attain if one of the coefficients C0-C5 is equal to unity and the others zero.	6F10.5
4	Z1 - Starting point of integration measured from coordinate system at centre of multipole element (cm). Normally negative. Z2 - Termination point of integration measured from coordinate system at centre of multipole element (cm). Normally positive.	2F10.5
5	C0 - Coefficients describing dipole, quadrupole, etc. C1 content of the field. Normal range -1. to +1. C2 C3 C4 C5	6F10.5
6	C6 - Not used. C7 - Coefficients used to define how the field varies with z/L , basically describing a bell-shaped curve. Typical values are C7=0.4, and C8=0.1 C8	3F10.5

F. Solenoid (4 records)

<u>Record</u>	<u>Variable</u>	<u>Format</u>
1	SOLE	A4
2	LF - Integration step size (cm) for all regions. Recommended: $LF=0.2D$	F10.5
3	A - Distance (cm) from origin of system A (initial) to the entrance edge of the solenoid element (i.e., edge of the hardware, not the EFB). B - Distance (cm) from exit edge of the solenoid element to origin of output system D L - Length (cm) of solenoid. D - Diameter (cm) of solenoid. BF - Asymptotic magnetic field of solenoid (Tesla), i.e. $BF = 0.4\pi IN/L$	5F10.5
4	Z11 - Starting point of integration measured from input edge of solenoid. Normally positive. Z22 - Termination point of integration measured from exit edge of solenoid. Normally positive.	2F10.5

G. Velocity Selector (11 records)

Record	Variable	Format
1	VELS	A4
2	LF1 - Integration step size (cm) of the entrance fringing field region. LU1 - Uniform field integration step size (cm). LF2 - Exit fringing field integration step size (cm). DG - Differential step size (cm) used in determining off mid-plane components of E and B using a numerical differential technique. Recommended: LF1=LF2=0.3DE; LU1 can be larger; DG=0.2DE or smaller.	4F10.5
3	A - Distance (cm) from origin of system A (initial) to system B (situated at EFB of entrance fringing field) B - Distance (cm) from origin of system C (situated at exit edge EFB of velocity selector) to origin of output system D. L - Effective length (cm) of velocity selector. BF - Magnetic field of velocity selector (Tesla)= B_y . EF - Electric field of velocity selector (kV/cm)= E_x .	5F10.5
4	RB - Equivalent radius required if $NDX \neq 0$. NDX - First order magnetic field index	2F10.5
5	DB - Separation distance of magnetic poles (cm). DE - Separation distance of electrodes (cm). WB - Width of magnetic poles (cm). WE - Width of electrodes (cm).	4F10.5
6	Z11 - Integration limit (cm) defining the start of the entrance fringing field zone in coordinate system B. Normally positive. Z12 - Integration limit (cm) defining the termination of the entrance fringing field zone in coordinate system B. Normally negative. Z21 - Integration limit (cm) defining the start of the exit fringing field zone in coordinate system C. Normally negative. Z22 - Integration limit (cm) defining the termination of the exit fringing field zone in coordinate system C. Normally positive.	4F10.5

G. Velocity Selector (11 records) - Continued

Record	Variable	Format
7	BC2 - Coefficients describing second and fourth order BC4 iso-field lines on the median plane in the fringing EC2 field region due to finite width of magnetic poles EC4 and electrodes.	4F10.5
8	CB0 - Coefficients used in the expansion of the CB1 magnetic fringing field fall-off at the entrance CB2 of the velocity selector. CB3 CB4 CB5	6F10.5
9	CE0 - Same as CB coefficients, but for the electric CE1 fringing field. CE2 CE3 CE4 CE5	6F10.5
10	CB10 - Same as CB coefficients, but for the magnetic CB11 fringing field at the exit. CB12 CB13 CB14 CB15	6F10.5
11	CE10 - Same as CE coefficients, but for the electric CE11 fringing field at the exit. CE12 CE13 CE14 CE15	6F10.5

H. Lens (3 records)

<u>Record</u>	<u>Variable</u>	<u>Format</u>
1	LENS	A4
2	X/X - Matrix elements for the spatial coefficients X/T of the transformation matrix of an arbitrary T/X element. Units for lengths and angles are cm T/T and mr, respectively. Particularly useful for an Y/Y electrostatic Einzel lens, for instance, in an Y/P otherwise magnetic optical system. P/Y Note: the time variable t used in RAYTRACE is P/P not updated through LENS even if the coefficients X/T and Y/P are used to describe a finite thickness.	8F10.5
3	CS - Correction term for spherical aberration. E0 - Reference energy for chromatic correction to focal length. N - Index for chromatic focal length correction.	3F10.5

I. Shift-Rotate (2 records)

<u>Record</u>	<u>Variable</u>	<u>Format</u>
1	SHRT	A4
2	<div>X0 - All following coordinate systems are displaced in the x-direction by an amount X0 (cm) as measured in the preceding system.</div> <div>Y0 - All following coordinate systems are displaced in the y-direction by an amount Y0 (cm) as measured in the preceding system.</div> <div>Z0 - All following coordinate systems are displaced in the z-direction by an amount Z0 (cm) as measured in the preceding system.</div> <div>ψ_x - The rest of the optical system as a unit is rotated ψ_x (degrees) about the x-axis of the preceding system.</div> <div>ψ_y - The rest of the optical system as a unit is rotated ψ_y (degrees) about the y-axis of the preceding system.</div> <div>ψ_z - The rest of the optical system as a unit is rotated ψ_z (degrees) about the z-axis of the preceding system.</div>	6F10.5

J. Drift (2 records)

<u>Record</u>	<u>Variable</u>	<u>Format</u>
1	DRIF	A4
2	DZ - Field free drift length (cm)	F10.5

K. Collimator (2 records)		
<u>Record</u>	<u>Variable</u>	<u>Format</u>
1	COLL	A4
2	J - Shape index. J=0, rectangular collimator J=1, elliptical collimator X0 - <i>x</i> -coordinate of collimator center Y0 - <i>y</i> -coordinate of collimator center XMAX - Half-axis in the <i>x</i> -direction YMAX - Half-axis in the <i>y</i> -direction	5F10.5

L. System End (1 record)

<u>Record</u>	<u>Variable</u>	<u>Format</u>
1	SENT - Record separating input data defining the magnetic elements of the system from the data specifying the input coordinates of the different rays to be traced through the system.	A4

M. Input Rays

A. Individual Rays (JNR=0, NR records)

Record	Variable	Format
1→NR	<p>XI - Particle x-coordinate (cm) at origin of system A for the first element.</p> <p>VXI - Angle (mr) of particle trajectory projected on xz-plane.</p> <p>YI - Particle y-coordinate (cm) at origin of system A for the first element.</p> <p>VYI - Angle (mr) of particle trajectory projected on yz-plane.</p> <p>ZI - Particle z-coordinate (cm) at origin of system A for the first element.</p> <p>VZI - Not used</p> <p>DELE - Kinetic energy deviation (%) of particle from central energy</p>	7F10.5

B. Program-generated rays (JNR≠0. One or more records)

Record	Variable	Format
1	<p>TMIN - Paraxial midplane angle (mr) for Ray 2.</p> <p>PMIN - Paraxial transverse plane angle (mr) for Ray 2.</p> <p>XMAX - For JNR≠46, common x-axis displacement for all rays. For JNR=46, maximum non-point source midplane deviation.</p> <p>TMAX - Maximum angle (mr) defining midplane solid angle</p> <p>YMAX - For JNR≠46, common y-axis displacement for all rays. For JNR=46, maximum non-point source transverse plane deviation.</p> <p>PMAX - Maximum angle (mr) defining transverse plane angle.</p> <p>DMAX - For JNR≠46, common energy deviation (%) for all rays. For JNR=46, maximum energy deviation (%) defining longitudinal phase space acceptance.</p>	7F10.5
2→(NR-JNR)	<p>Any number of input records defining individual rays can be added to the single line for program-generated rays. NR must be set equal to the total number to be traced.</p>	

Appendix 2. Samples of Input Data Files

A. Magnetic Dipole, MTYP=2.

FILE: DIPOLE.DAT HAE 4/16/86

03, 500, 0, 2, 0, 00, 01

300., 10., 1.

DIPOLE D1

3., 10., 3., 1., 2.

200., 200., 10., 100., 1.000

90., 27., 27.

0.

40., -20., -20., 40.

.2401, 1.8369, -.5572, .3904

.2401, 1.8369, -.5572, .3904

0.

0.

1., -2., 0., 0., 0., 0.

1., 2., 0., 0., 0., 0.

SENTINEL

0.

0., 20.

0., -20.

2., 1., 0., 25., 0., 20.

B. Electrostatic Deflector

FILE: EDIPL.DAT - ELECTROSTATIC DEFLECTOR - HAE 2/26/86

1, 100, 0, 2, 0, 00, 00,

5., 1., 1., 200., 1.0,

SHRT

-.1

EDIPOLE

.5 ,.5 ,.5 ,.5

25., 25., 4., 100., 100.

10.,

.3, .1, 10., 0.,

8., -5., -5., 8.,

.3813, 1.6370, -.64083, .36664, 0., 0.,

.3813, 1.6370, -.64083, .36664, 0., 0.,

SHRT

.1

SENTINEL

0.

C. Pretzel Magnet

FILE: PRETZEL.DAT HAE 3/16/85

3, 500, 0, 2, 0, 00, 01

5., 5., 3., 100., 10.

DIPOLE D2

2., 2., 2., -.2, 6.

75., 75., 10., 0., 1.

270., 45., 45.

.806

0.

0.

0.

0.

0.

0.

0.

SENTINEL

0.

1.

0., 0., 1.

COMMENTS:

1. FREE-FLOATING FORMAT WITH COMMAS APPROPRIATE FOR VAX COMPUTER
2. THE DIGIT 2 IN RECORD 2 PRODUCES OUTPUT IN THE D-AXIS SYSTEM
3. LAST DIGIT 1 IN RECORD 2 CREATES A PLOT FILE
4. DG=-.2 (RECORD 5) IS APPROPRIATE FOR PRETZEL MAGNETS ONLY. SEE TEXT.
5. R=0 (RECORD 6) IS APPROPRIATE FOR PRETZEL MAGNETS ONLY

D. Clamshell Spectrometer

QCLAM - U of I P=400 MeV/c (alpha=beta=-7) 10/20/84.

03, 500, 0, 0, 0, 00, 01

360., 40., 3.

POLES

4., 4., 4.

50., 37., 50., 12.0

-.474, .142, .081, .028, .015

30., -18., -18., 30.

.1122, 6.2671, -1.4982, 3.5882, -2.1209, 1.723

.1122, 6.2671, -1.4982, 3.5882, -2.1209, 1.723

0.9, 0.8, 0.7, 0.6, .025, .050, .075, .10,

SHRT

0., 0., 0., 0., -60.

DIPOLE

4., 8., 4., 1., 4.

0., 0., 15.00, 133333., 1.6062

.0371, -67., 0.

804.

60., -40., 0., 0.

.2401, 1.8639, -.5572, .3904

-10., 0., 0., 0.,

0.

0.

530., -3.12E6, 5.9E9, -4.0E12,

0.

DIPOLE

4., 8., 4., 1., 4.

0., 0., 15.00, 133333., 1.6062

.0371, 0., -67.

804.

0., 0., -40., 60.

-10., 0., 0., 0.,

.2401, 1.8639, -.5572, .3904

0.

0.

0.

-483., 1.0E5, -1.0E8, -2.0E11, 1.E14

SHRT

0., 0., 0., 0., -60.

DRIFT

120.

SENTINEL

0.,

0., 100.

0., -100.

10., 1., 0., 100., 0., 100.

.5, 0., 0., 0., 0., 0., .086

.5, 100., 0., 0., 0., 0., .086
.5, -100., 0., 0., 0., 0., .086

